University of Illinois at Urbana-Champaign

ACRC

Air Conditioning and Refrigeration Center A National Science Foundation/University Cooperative Research Center

Evaporation Heat Transfer and Pressure Drop in Ozone-Safe Refrigerants and Refrigerant-Oil Mixtures

J. S. Panek, J. C. Chato, J. M. S. Jabardo,
A. L. de Souza and J. P. Wattelet

ACRC TR-11 January 1992

For additional information:

Air Conditioning and Refrigeration Center
University of Illinois
Mechanical & Industrial Engineering Dept.
1206 West Green Street
Urbana, IL 61801

(217) 333-3115

Prepared as part of ACRC Project 01
Refrigerant-Side Evaporation and Condensation Studies
J. C. Chato, Principal Investigator

The Air Conditioning and Refrigeration Center was founded in 1988 with a grant from the estate of Richard W. Kritzer, the founder of Peerless of America Inc. A State of Illinois Technology Challenge Grant helped build the laboratory facilities. The ACRC receives continuing support from the Richard W. Kritzer Endowment and the National Science Foundation. The following organizations have also become sponsors of the Center.

Acustar Division of Chrysler
Allied-Signal, Inc.
Amana Refrigeration, Inc.
Bergstrom Manufacturing Co.
Caterpillar, Inc.
E. I. du Pont de Nemours & Co.
Electric Power Research Institute
Ford Motor Company
General Electric Company
Harrison Division of GM
ICI Americas, Inc.
Johnson Controls, Inc.
Modine Manufacturing Co.
Peerless of America, Inc.
Environmental Protection Agency
U. S. Army CERL
Whirlpool Corporation

For additional information:

Air Conditioning & Refrigeration Center
Mechanical & Industrial Engineering Dept.
University of Illinois
1206 West Green Street
Urbana, IL 61801

217 333 3115

Abstract

The ozone-depleting effect of chlorofluorocarbons (CFC's) has caused an intensive search for alternative fluids to be used in vapor-compression refrigeration and air-conditioning machinery. A promising replacement for CFC-12 has been identified, hydro-fluorocarbon (HFC) 134a. This new refrigerant is expected to have different heat transfer and pressure drop characteristics than CFC-12 when changing phase in the evaporator component. The presence of oil for lubrication purposes may also have an effect. Heat transfer coefficients and pressure drops of HFC-134a and CFC-12 boiling in horizontal tubes were measured. Polyalkylene Glycol (PAG) and Ester oils were mixed with HFC-134a to determine effects of various concentrations of oil. Tests were run in the mobile air-conditioning range of temperature (5°C), mass fluxes (100 to 500 kg/m^2s), and heat fluxes (5 to 30 kW/m^2). Various inlet qualities to the test section were studied, from 20 to 60 percent. Comparison of data with previous correlations from the literature is made, and a new correlation for pure refrigerant heat transfer is proposed.

Table of Contents

List of Figure

Page

List of Tables

Page

Nomenclature

c_1-c_4	constants in Kandlikar correlation	
C	intermediate variable in Tichy correlation	
c_p	specific heat at constant pressure	[J/kg-K]
D	diameter	[m]
g	gravitational constant	[9.8 m/s^2]
G	mass flux	[kg/s-m^2]
h	convective heat transfer coefficient	[W/m^2-K]
i	enthalpy	[J/kg]
k	thermal conductivity	[W/m-K]
K_1-K_2	constants in Tichy correlation	
$\dot{m}$	mass flow rate	[kg/s]
M_1-M_3	weights used in oil concentration measurement	[kg]
$\dot{q}$	heat power rate	[W]
T	temperature	[°C]
x	thermodynamic quality	

Greek Symbols

β	contact angle	[degrees]
χ_{tt}	Lockhart-Martinelli parameter	$[(\frac{1-x}{x})^{0.9}(\frac{\rho_g}{\rho_l})^{0.5}(\frac{\mu_l}{\mu_g})^{0.1}]$
ϕ	heat flux	[W/m^2]
μ	dynamic viscosity	[Ns/m^2]
ρ	density	[kg/m^3]
σ	surface tension	[N/m]
ω_o	oil concentration	[kg_o/kg_{ref}]

Dimensionless Groups

Bo	Boiling number	[ϕ/Gi_{fg}]
Co	Convection number	$\left(\frac{1-x}{x}\right)^{0.8}\left(\frac{\rho_g}{\rho_l}\right)^{0.5}$
Fr	Froude number	[$G/\rho_l^2 gD$]
Ja	Jacob number	[$c_p(T_{wall}-T_{sat})/i_{fg}$]
Nu	Nusselt number	[hD/k]
Pr	Prandtl number	[$c_p\mu/k$]
Re	Reynolds number	[GD/μ]

Subscripts

b	bulk
fg	vaporization latent quantity
g	gas
in	inlet

l	liquid portion ($G_l = G_{tp}(1-x)$)
lo	entire mixture flowing as a liquid only ($G_{lo} = G_{tp}$)
mix	mixture of refrigerant and oil
o	oil
ph	preheater
ref	refrigerant
sat	saturation condition
tp	two-phase, vapor and liquid mixed together
ts	test section
v	vapor
wall	internal tube wall surface contacting the refrigerant

Chapter 1: Introduction

Stratospheric ozone absorbs the Sun's high energy ultra-violet rays and prevents them from reaching ground levels where they would interact harmfully with both animal and plant life. A growing body of evidence shows that this protective layer of ozone is being depleted. Measurements by high flying planes, balloons, and satellites have shown severe depletion in polar regions and smaller reductions of stratospheric ozone levels globally. Much research has been done to determine the cause of this ozone depletion, and the general consensus is that free chlorine radicals act as catalysts for the chemical degradation of ozone into normal oxygen molecules. Other chemicals such as bromine can also promote the degradation of ozone.

The presence of chlorine in the stratosphere is believed to be the result of migration of chlorine-containing chemicals. These chemicals have long lifetimes before being broken down into their elemental constituents. This long lifetime allows them to be carried over time into the stratosphere, where they eventually break down and release chlorine. A large class of chemicals which behaves in this manner are the chlorofluorocarbons (CFC's). These chemicals are widely used by both consumers and industries around the world due to their nonflammability, low toxicity, and material compatibility. CFC's are commonly used as refrigerants, solvents, and blowing agents for foams.

The replacement of CFC's by ozone-safe chemicals is a daunting task, simply because of the large amounts being produced and used. However, in 1987 an international group of government officials and scientists met to formulate the Montreal Protocol. This agreement called for halving the use of CFC's by 1998. A Revised Montreal Protocol was enacted in 1990, and calls for a 50% cut by 1995, an 85% cut in 1997, with complete phaseout of CFC's by 2000. In addition to CFC's, other chlorine containing compounds such as carbon tetrachloride and methyl chloroform are addressed in the latest protocol [Aldhous, 1990].

Since the initial discovery of ozone depletion, corporations have been looking for replacements for CFC's. An alternative to CFC-12 has been identified, hydrofluorocarbon 134a (HFC-134a). HFC-134a is a promising replacement in the refrigerant application because its saturation pressure is very similar to that of CFC-12 in the temperature range of most refrigeration and air-conditioning applications. However, other properties of HFC-134a must be studied before it can replace CFC-12.

Since most refrigeration systems operate with a vapor compression cycle, they require a small amount of lubricating oil to be mixed with the refrigerating fluid. This oil is absolutely necessary to lubricate sliding surfaces in the compressor. The compatibility of HFC-134a with various oils is one of the characteristics that has been researched. Another property of HFC-134a that must be investigated is how well it transfers heat during evaporation and condensation in the vapor compression refrigeration cycle.

The purpose of our project is to investigate experimentally the evaporating heat transfer and pressure drop characteristics of ozone safe refrigerants. The work is performed at the Air Conditioning and Refrigeration Center (ACRC) of the University of Illinois at Urbana-Champaign. A test apparatus has been constructed which allows measurement of evaporative heat transfer coefficients and pressure drops of refrigerants flowing in horizontal tubes. This testing system can control mass fluxes, heat fluxes, entering qualities, oil concentrations, and saturation temperatures of refrigerants flowing in smooth or enhanced tubes of various sizes and geometries. Flow conditions

corresponding to both refrigeration and air conditioning modes can be set. Up to 48 channels of data can be input to the microcomputer controlled data acquisition system, keeping track of various temperatures, pressures, electrical powers, and flow rates in the test loop.

This thesis describes the comprehensive series of tests run with HFC-134a and CFC-12 in the air conditioning temperature range. Mixtures of HFC-134a and various oils were also tested to determine oil effects on heat transfer and pressure drop. The rest of this thesis will describe in detail the test system components, operating procedures, data acquisition and reduction, results of work performed, and recommendations for future work.

Chapter 2 is a literature survey of past and recent work on boiling refrigerants and their oil mixtures. Chapter 3 contains a detailed description of the test apparatus and instruments. Chapter 4 describes data acquisition hardware and software as well as data reduction techniques and software. Chapter 5 contains the test plan, outlining the different parameters varied to obtain a full test matrix. This includes HFC-134a and CFC-12 test runs at the mobile air conditioning temperature condition. Results of experimental test runs are presented and discussed. The graphs presented show the effect of varying parameters in the tests. Chapter 6 is a comparison of the data with previously proposed correlations in the open literature. A new correlation for the data is proposed. Chapter 7 contains conclusions drawn from the current research. Specific suggestions are made for future work and for design of system components.

The appendices contain detailed procedures for test loop start up, operation, and shut down, oil concentration measurement, and oil charging and flushing techniques. Tables for the complete set of data obtained are also included.

Chapter 2: Literature Review

Evaporation of refrigerants is a well studied research area. Papers dealing with the evaporation of different types of pure refrigerants, refrigerant mixtures containing oil, tube geometries, and tube enhancements can be found in the open literature. This literature review will summarize some works which focus on the investigation of heat transfer coefficients of CFC-12 or HFC-134a and their oil mixtures in horizontal smooth tubes. These papers present the heat transfer coefficients and some propose correlations based on their experimental data.

2.1. Heat Transfer Characteristics of Pure Refrigerants

Most of the correlations proposed define a ratio of two-phase heat transfer coefficient to single-phase liquid heat transfer coefficient, h_{tp}/h_l or h_{tp}/h_{lo}. Unless noted otherwise, all correlations discussed in this literature review assume the single-phase coefficient to be that of the commonly used Dittus-Boelter (1930) correlation:

$$h_l = 0.023 \frac{k_l}{d}\left(\frac{G(1-x)D}{\mu_l}\right)^{0.8}\left(\frac{c_{pl}\,\mu_l}{k_l}\right)^{0.4} \tag{2.1a}$$

$$h_{lo} = 0.023 \frac{k_l}{d}\left(\frac{G\,D}{\mu_l}\right)^{0.8}\left(\frac{c_{pl}\,\mu_l}{k_l}\right)^{0.4} \tag{2.1b}$$

Chaddock and Noerager (1966) performed experiments with CFC-12 in a conventional refrigeration cycle, using an electrically heated steel tube for the evaporator. Evaporation temperature was 54°F (12.2°C), and local heat transfer coefficients were measured. A small amount of oil was present in their system despite the use of oil separators. They proposed two equations based on the Lockhart-Martinelli parameter which correlate their results within ± 20%:

$$\frac{h_{tp}}{h_{lo}} = \frac{3.0}{(\chi_{tt})^{2/3}} \tag{2.2}$$

and

$$\frac{h_{tp}}{h_l} = \frac{3.0}{\chi_{tt}} \tag{2.3}$$

Kandlikar (1987) gathered over 5000 data points on evaporative heat transfer of different fluids from different researchers. He proposed a general correlation which has a mean deviation of 18.8% for refrigerant data. One notable feature is that of a fluid dependent parameter which can be estimated from pool boiling data. This allows prediction of flow boiling heat transfer coefficients based on experimental pool boiling data. The final form of the correlation for horizontal flow with $Fr_l > 0.04$ is:

$$\frac{h_{tp}}{h_l} = c_1\, Co^{c2} + c_3\, Bo^{c4}\, F_{fl} \tag{2.4}$$

Table 2.1. Constants in Kandlikar Correlation

Constants	Convective Region (Co < 0.65)	Nucleate Boiling Region (Co > 0.65)
c1	1.1360	0.6683
c2	-0.9	-0.2
c3	667.2	1058.0
c4	0.7	0.7

Table 2.2. Fluid Parameter F_{fl} in Kandlikar Correlation

Fluid	F_{fl}	Fluid	F_{fl}
Water	1.00	CFC-113	1.10
CFC-11	1.30	CFC-114	1.24
CFC-12	1.50	HFC-152a	1.10
CFC-13B1	1.31	Nitrogen	4.70
HCFC-22	2.20	Neon	3.50

To use the Kandlikar correlation to calculate the heat transfer coefficient for any given condition, Equation 2.4. is calculated using both sets of coefficients c_1-c_4. The higher of the heat transfer coefficients calculated is the one predicted by the correlation.

Jung, McLinden, Radermacher, and Didion (1989) studied local heat transfer coefficients in boiling mixtures of CFC-12 and HFC-152a. Analysis of over 2000 data points resulted in correlations with mean deviations of 7.2% for pure refrigerants and 9.6% for mixtures. The correlation for pure refrigerants is:

$$h_{tp} = N\, h_{sa} + F_p\, h_l \tag{2.5}$$

where

$$N = 4048\, \chi_{tt}^{1.22}\, Bo^{1.13} \quad \text{for } \chi_{tt} < 1.0 \tag{2.6}$$

and h_{sa} is the nucleate pool boiling heat transfer coefficient predicted by the Stephan and Abdelsalam (1980) correlation:

$$h_{sa} = 207 \frac{k_l}{bd} \left(\frac{q\, bd}{k_l\, T_{sat}} \right)^{0.745} \left(\frac{\rho_v}{\rho_l} \right)^{0.581} Pr^{0.533} \tag{2.7}$$

$$bd = 0.0146\, \beta \left(\frac{2\sigma}{g(\rho_l - \rho_v)} \right)^{0.5} \tag{2.8}$$

$$\beta = 35° \text{ (contact angle typical for refrigerants)} \tag{2.9}$$

$$F_p = 2.37 \left(0.29 + \frac{1}{\chi_{tt}} \right)^{0.85} \tag{2.10}$$

Eckels and Pate (1990) compared heat transfer coefficients of HFC-134a to CFC-12 in liquid single phase cooling, evaporation, and condensation tests. They used a counter-flow water annulus to heat or cool the refrigerant, and the refrigerant was circulated using a liquid pump instead of a vapor compressor. They found that

heat transfer coefficients for HFC-134a are 40% higher in evaporation and 30% higher in condensation than for CFC-12, based on equivalent mass fluxes and quality changes in the test section. A 33% increase in heat transfer coefficient for HFC-134a was observed in single phase liquid cooling tests. They also compared heat transfer coefficients based on equivalent cooling capacities. Since HFC-134a has a higher heat of vaporization, a given cooling capacity for HFC-134a would have a lower flow rate than CFC-12. The ratio of flow rates of the two refrigerants is inversely proportional to the ratio of enthalpies of vaporization. The heat transfer coefficients were still higher for HFC-134a by 5% to 20% over CFC-12.

Takamatsu, Momoki, and Fujii (1991) studied HFC-134a and CFC-12 evaporation in a test section heated by an annular water flow. They recorded local heat transfer coefficients, and found that HFC-134a has 25% higher coefficients than CFC-12 at the same saturation temperature, mass velocity, heat flux, and quality. Some investigation of a test section accidently fouled by naphthenic oil residues was also done, with the result of coefficients up to 100% higher than a clean tube. It is also interesting to note their relatively high evaporating temperature of 77°F (25°C).

XingXi, Xinqiao, Dazhong, and Chibin (1991) measured CFC-12 evaporating at -13°F (-25°C). Two electrically heated test sections were used, an instrumented copper tube and a metal film coated glass tube, in order to study both flow patterns and actual heat transfer characteristics. They proposed a correlation for heat transfer coefficient based on the Lockhart-Martinelli parameter:

$$\frac{h_{tp}}{h_{lo}} = \frac{5.1176}{(\chi_{tt})^{0.1689}} \qquad (2.11)$$

Jung and Radermacher (1991) measured local evaporative heat transfer coefficients for pure CFC-11 and HFC-134a and found them to be within a mean deviation of 7% of the earlier correlation presented by Jung et al. (1989). Based on equivalent cooling capacities, HFC-134a was found to have a heat transfer coefficient from 10% to 12% higher than that of CFC-12.

Wattelet et al. (1991) tested pure CFC-12 and HFC-134a evaporating in a test section heated by longitudinally wrapped strip heaters. Temperatures for evaporation were 40°F (4.4°C) and inlet qualities were 20% in all cases. Liquid refrigerant was circulated by a gear pump. Heat transfer coefficients for HFC-134a were 10% to 40% higher than for CFC-12 at identical conditions. Wattelet proposed two correlations which match his data to within ±7% for CFC-12 and within ±8% for HFC-134a:

$$\frac{h_{tp}}{h_{lo}} = \frac{2.3}{(\chi_{tt})^{0.666}} \qquad \text{(for CFC-12)} \qquad (2.12a)$$

and

$$\frac{h_{tp}}{h_{lo}} = \frac{2.9}{(\chi_{tt})^{0.666}} \qquad \text{(for HFC-134a)} \qquad (2.12b)$$

2.2. Heat Transfer Characteristics of Refrigerant-Oil Mixtures

Oil is included in most refrigeration systems to lubricate sliding metal surfaces in the compressor. This oil may migrate through the system and reach the evaporator section. The presence of oil in the refrigerant may have a significant influence on the flow pattern, pressure drop, and heat transfer in the evaporator component. These characteristics are affected because properties of the refrigerant such as surface tension, viscosity, and thermal conductivity change with the addition of oil.

Green and Furse (1963) studied CFC-12 mixed with "wax-free" oil boiling at 10°F (-12.2°C) to 40°F (4.4°C) in a heat-pipe type of apparatus. The test section was heated by condensing CFC-11 on the outer surface of the tube. They found that the average heat transfer coefficient for oil mass percentages of 0% to 8% is larger than the average heat transfer coefficient for the pure CFC-12 case. The highest heat transfer coefficient was obtained with 4% oil mass percentage.

Chaddock (1976) explains how oil affects the mixture properties and therefore the heat transfer, pressure drop, and flow pattern characteristics. He summarizes the results of previous studies of both flow and pool boiling and proposes a set of conclusions very useful for evaporator designers.

Tichy, Duval, and Macken (1986) measured local heat transfer coefficients of evaporating CFC-12 mixed with a naphthenic base lubricant of viscosity 300 SUS. Their test section used a water annulus to boil the CFC-12, and also included three viewing ports for flow visualization. At low qualities and low wall superheat, the presence of oil was found to enhance heat transfer, while at higher qualities the heat transfer was degraded. They proposed a correlation which is valid over a large quality range and for several flow patterns. The equation represents 85% of the data within 35%:

$$Nu_{tp} = Nu_{DB}\, C(\chi_{tt}, Ja, \omega_o) \tag{2.13}$$

where Nu_{DB} is the Dittus-Boelter Nusselt number:

$$Nu_{DB} = 0.023\, Re_l^{0.8}\, Pr_l^{0.4} \tag{2.14}$$

and

$$\log_{10} C = \frac{K_1}{(\log_{10}\chi_{tt} - K_2)} \tag{2.15}$$

$$K_1 = K_{1a}(\omega_o) - K_{1b}(\omega_o)\, log_{10} Ja \tag{2.16}$$

$$K_2 = K_{2a}(\omega_o) - 2\, log_{10} Ja \tag{2.17}$$

and K_{1a}, K_{1b}, and K_{2a} are constants that depend on ω_o, given in Table 2.3.

Table 2.3. Constants in Tichy Correlation

ω_o	K_{1a}	K_{1b}	K_{2a}
0.0	3.79	0.21	-9.0
0.02	3.56	1.34	-11.0
0.05	2.17	3.01	-13.0

Spatz and Zheng (1990) measured evaporation and condensation heat transfer coefficients with CFC-12/mineral oil and HFC-134a/PAG oil mixtures. They used annular water flow to add and remove heat from the refrigeration system. They observed better heat transfer with the HFC-134a than with the CFC-12 in almost all cases. A 10 to 20% increase in evaporative heat transfer was reported with HFC-134a. Coefficients of performance of heat pumps using the two refrigerant/oil mixtures were similar.

Fukushima and Kudou (1990) measured local heat transfer coefficients in forced convection evaporation and condensation. A HFC-134a/PAG oil mixture and a CFC-12/mineral oil mixture were tested in a vapor compression type test circuit. Oil separation was performed in the oil-free test runs. They observed that local heat transfer coefficients rise gradually with increasing quality, until quality is approximately 0.90, and then drop rapidly. The presence of oil decreased average heat transfer coefficients by up to 20% with an oil mass fraction of 10%.

Hambraeus (1990) reported local heat transfer coefficients of an HFC-134a/oil mixture boiling in an electrically heated smooth tube. Sight glasses at four points in the test section allowed direct observation of the flow pattern. She reported that at low heat fluxes, a 20% increase in average heat transfer coefficient occurs when the oil content is 0.5%. At higher heat fluxes, a decrease in heat transfer coefficient is observed, up to 20% at 2% oil content.

A further study by Hambraeus (1991) describes the effects of oil viscosity on heat transfer coefficients of HFC-134a/oil mixtures. Two different oils were tested, with viscosities of 28.6 cSt and 123.9 cSt at 104°F (40°C). No differences in boiling heat transfer coefficients between the two refrigerant-oil mixtures were observed for high heat fluxes of 1900 to 2540 Btu/ft^{2}hr (6-8 kW/m^2). At low heat fluxes of 635 to 1270 Btu/ft^{2}hr (2-4 kW/m^2), small amounts of lower viscosity oil increased the heat transfer coefficient, while the higher viscosity oil always decreased the heat transfer coefficient.

Eckels and Pate (1991) studied average heat transfer coefficients in evaporation and condensation of HFC-134a/PAG oil and CFC-12/naphthenic oil mixtures. Oil concentrations were varied from 0% to 5.4% by mass. The test section was heated with a water annulus. For low PAG oil concentrations in HFC-134a, the average heat transfer coefficient was up to 10% greater than the pure HFC-134a runs. At oil concentrations of 5.4%, the average heat transfer coefficient was reduced by 40% to 50% from the pure HFC-134a runs. For CFC-12/naphthenic oil mixtures, a 5% to 8% increase in average heat transfer coefficient was observed at an oil concentration of 2.5%. At oil concentrations of 5.4%, the heat transfer coefficient was reduced by 40%.

2.3. Current Research in Heat Transfer of Pure Refrigerants and Refrigerant-Oil Mixtures

After reviewing the open literature on heat transfer characteristics of ozone-safe refrigerants, some gaps in available data are observed. Most of the work reported so far does not encompass the high flow rate and high heat flux conditions present in modern automotive air-conditioning systems. Another trend is toward measurement of some average heat transfer coefficient. More local measurements should be made so that two-phase flow phenomena such as wall dryout can be pinpointed.

The test apparatus described in this thesis will allow testing of ozone-safe refrigerants in flow regimes typically seen in automotive air-conditioning evaporators. Large amounts of data at different test conditions can quickly be obtained. As many as ten test runs have been recorded in a period of nine hours. The design of the

refrigerant loop allows rapid changeover to new test sections with different geometries or instrument locations. Reprogramming of the data acquisition software to accommodate new refrigerants and oils is possible in minutes. With the industry emphasis on short-term phase out of CFC's, this test apparatus can provide the large data base needed for efficient design of evaporators using the new refrigerants. The large amounts of data collected enables the correlation and prediction of evaporative heat transfer coefficients and pressure drops.

Chapter 3: Test Apparatus, Instrumentation, and Controls

A test apparatus has been constructed for the measurement of evaporative heat transfer coefficients and pressure drops of ozone safe refrigerants, shown in Figure 3.1. A refrigerant loop capable of investigating different refrigerants flowing in horizontal tubes is the main feature. A commercial R-502 chiller subsystem is thermally connected to the refrigerant loop to provide cooling. The test section can be easily isolated from the other test loop components to allow for quick repair or replacement.

In addition to the loop components, a full set of instruments measures temperatures, pressures, flow rates, and power levels at all important points in the various circuits. Control of heater power levels is by computer command. Refrigerant charge control is also described.

3.1. Test Apparatus

The test apparatus consists of the refrigerant flow loop, a commercial chiller subsystem, and the instrumented test section. A detailed description of start up, operating, and shut down procedures is given in Appendix A.

3.1.1. Refrigerant Flow Loop

The main component of the test apparatus is the refrigerant flow loop, shown in Figure 3.2. This loop is set up with the desired test section and charged with the refrigerant or refrigerant-oil mixture to be studied. Subcooled liquid exiting the condenser is pumped by a positive displacement gear pump into a radial piston type positive displacement flow meter. A bypass line connects the outlet of the pump back to the entrance of the condenser. This valved bypass allows coarse control of the mass flow rate into the test section. Once the refrigerant exits the flow meter, it enters the vertical circulation preheater. A precise amount of heat is added to boil the subcooled liquid. More heat is added in the test section to further vaporize the refrigerant. The outlet of the test section is connected to the two condenser modules, where the refrigerant is condensed and subcooled. The cycle then repeats.

Instrumentation is present at all important locations to give information on the state of the flowing refrigerant at that point. All sensors are wired directly to terminal panels mounted on the supporting framework, and are described in more detail in Section 3.2.

3.1.2. Ethylene Glycol / R-502 Chiller Loop

The chiller loop condenses and subcools the two-phase refrigerant flowing in the main loop. The main components of the chiller loop, shown in Figure 3.3., are the condenser modules, the ethylene glycol / water solution (brine) loop, the R-502 commercial chiller, and the system control panel.

The condenser modules are counterflow condensers, with refrigerant condensing on the outside of tubes which contain the circulating brine solution. Two modules are connected in parallel to provide adequate thermal capacity.

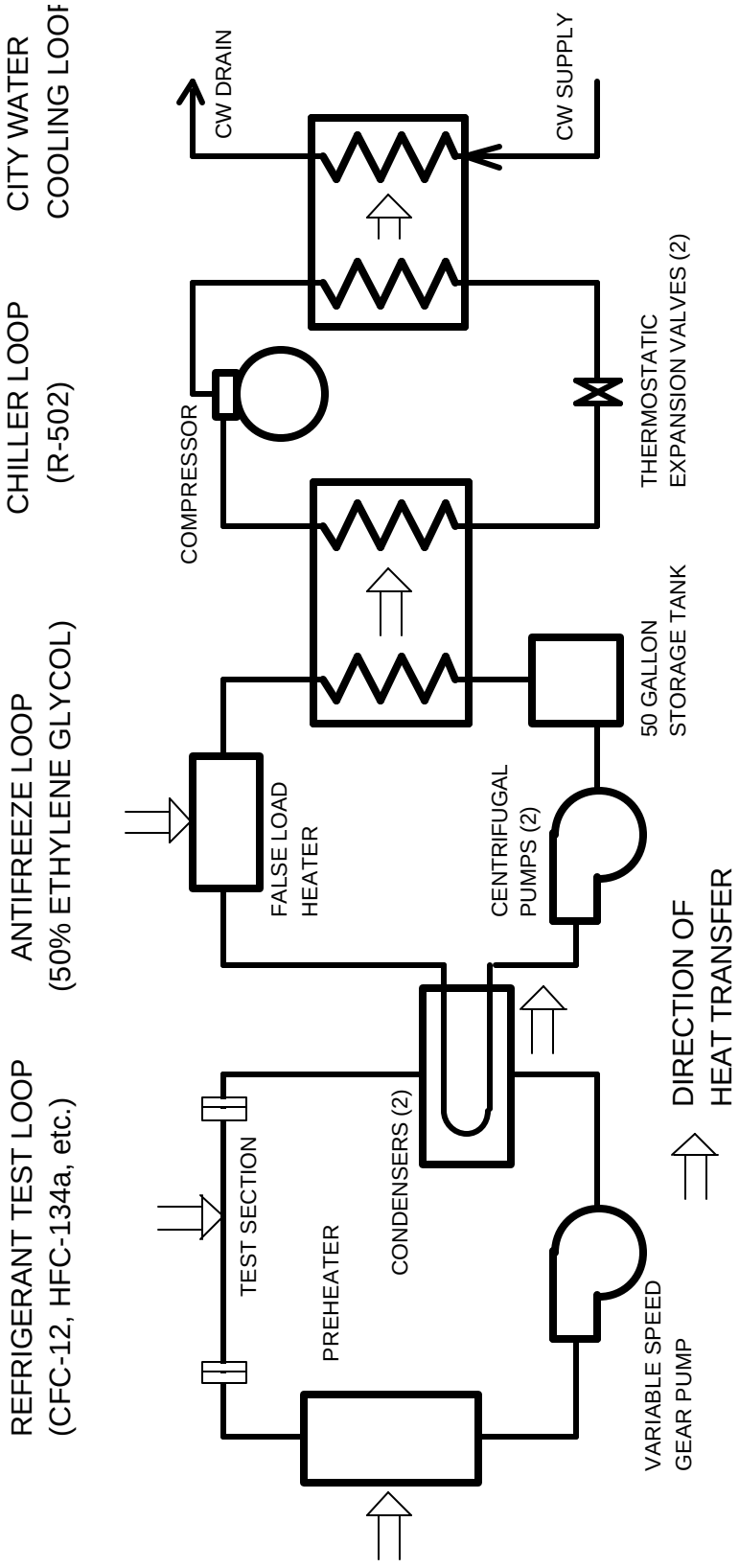

Figure 3.1. Test Apparatus

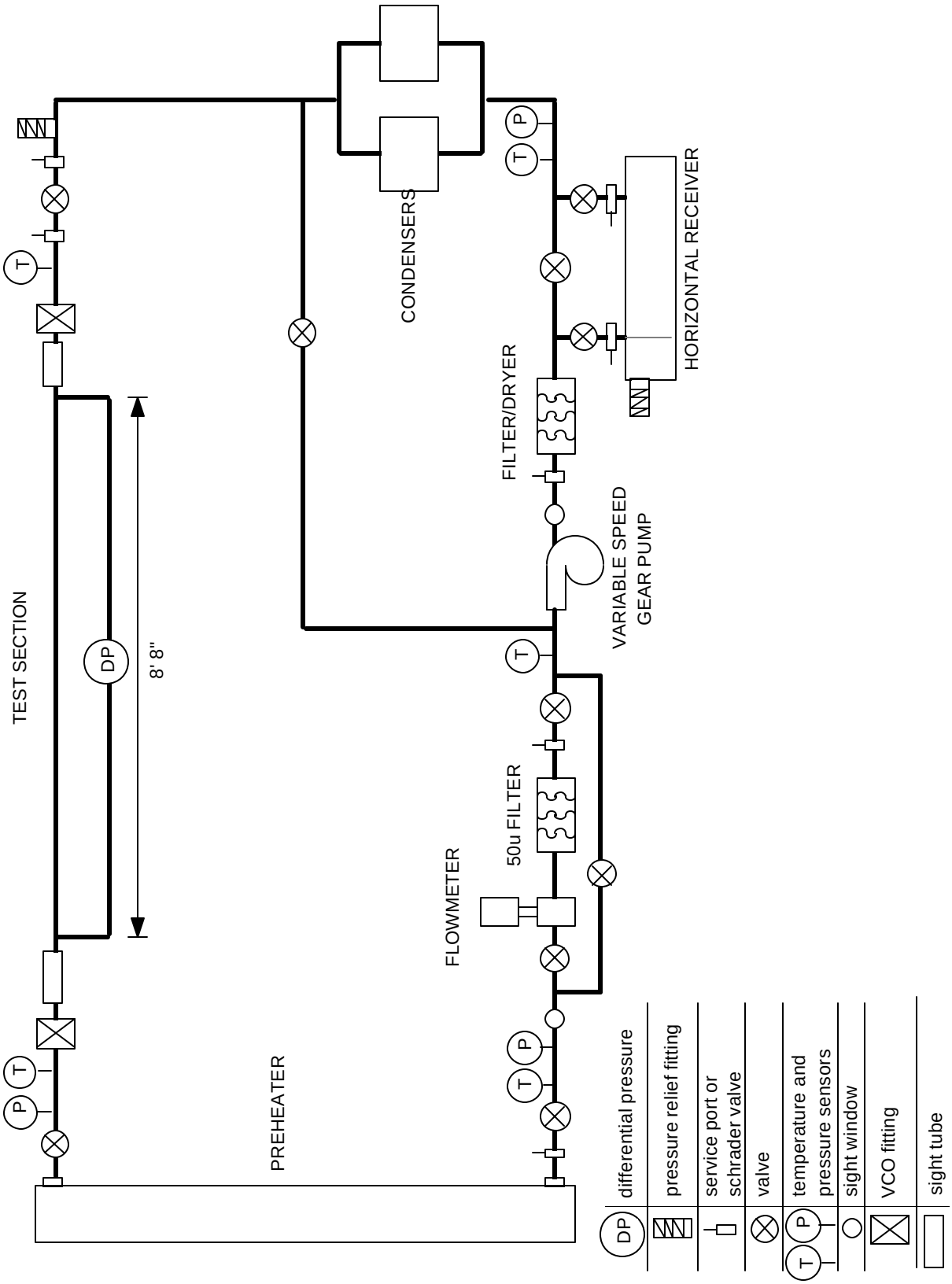

Figure 3.2. Refrigerant Test Loop

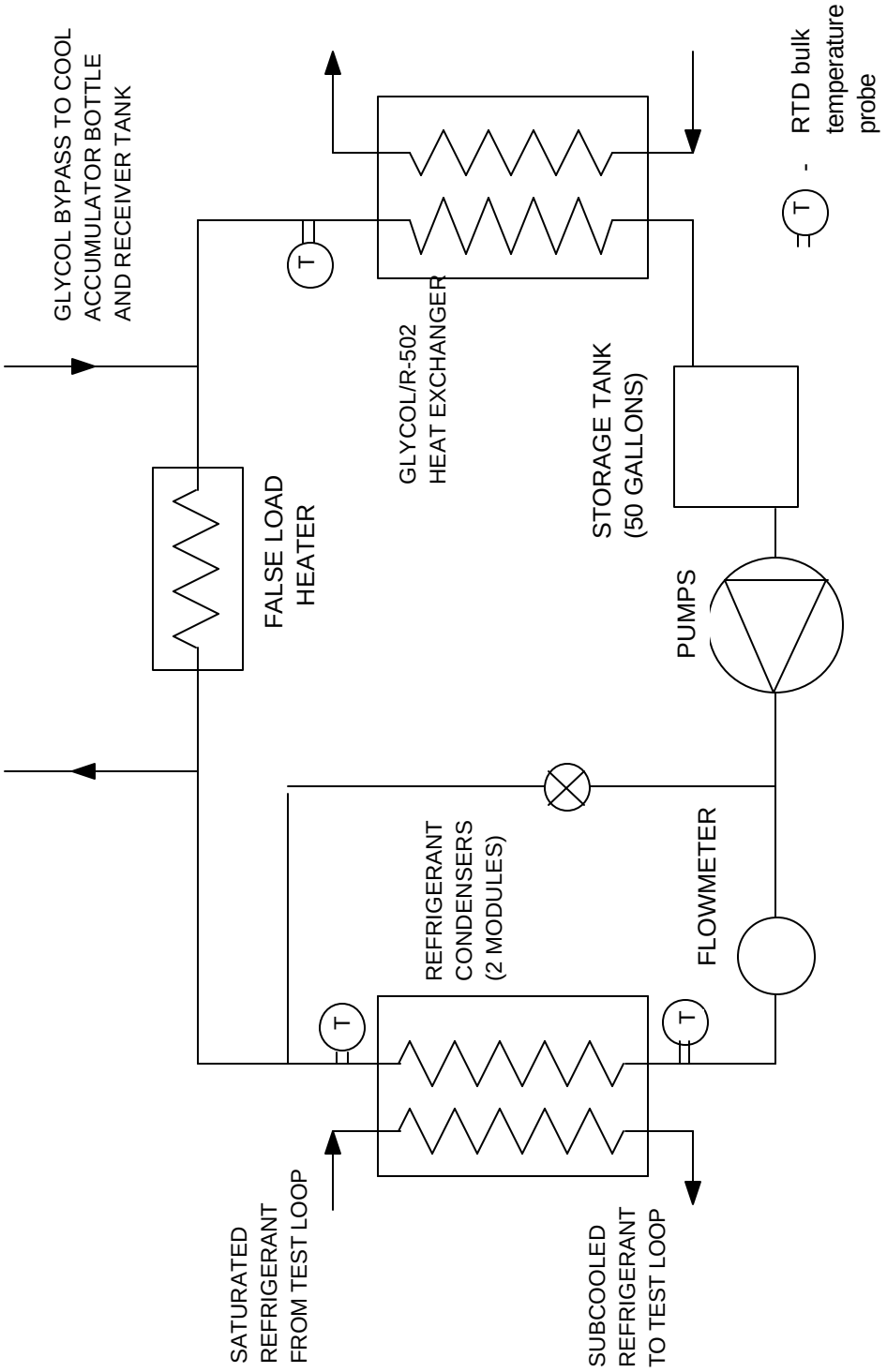

Figure 3.3. Chiller Loop

The brine loop consists of a 50 gallon storage tank, two centrifugal pumps connected in series, a turbine type flow meter, the two condenser shells, a 30,700 Btu/hr (9 kW) false load circulation heater, and the evaporator heat exchanger. The antifreeze mixture is pumped out of the storage tank, heated in the condensers and false load

heater, cooled by the R-502 system evaporator, and returned to the storage tank. Temperatures are measured in 3 locations to calculate energy balances against the main refrigerant loop.

The R-502 chiller is a custom built system assembled from various standard refrigeration components. The purpose of the chiller is to absorb heat from the brine loop and reject it to the city water coolant. Two separate thermostatic expansion valves are provided to allow high capacity at high temperatures, and somewhat lower capacity at lower temperatures. Experimental measurements of the capacity versus temperature of the solution at the condenser modules are shown in Figure 3.4.

The system control panel gives a display of current temperature of the antifreeze in the storage tank and setpoint temperature of chiller compressor. Three switches are on the control panel: master ON/OFF switch, antifreeze pump ON/OFF switch, and HI/LOW thermostatic valve selection switch.

Capacity control is accomplished by adjusting the compressor "ON" setpoint temperature artificially low. Then false load heat is added until the desired antifreeze temperature is attained. This somewhat wasteful method prevents cycling of the compressor around its setpoint temperature, minimizing temperature oscillations in the brine loop and the compressor wear caused by short cycling.

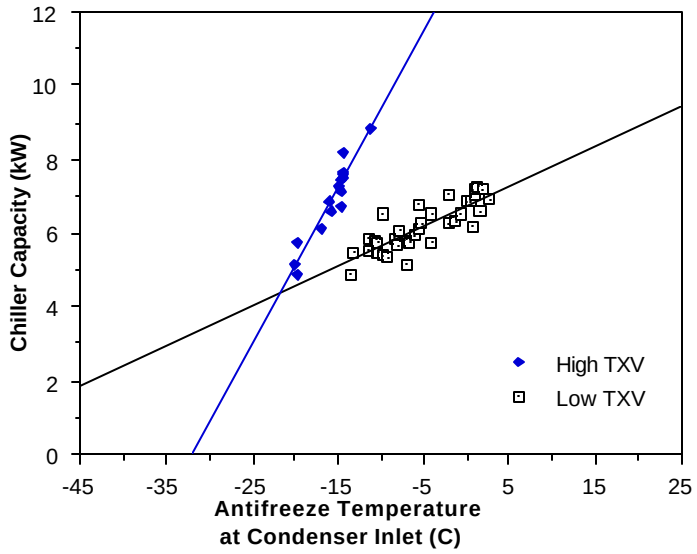

Figure 3.4. Chiller Capacity vs. Temperature

3.1.3. Test Section

The test section, shown in Figure 3.5, consists of a 0.500" O.D., 0.402" I.D. horizontal smooth copper tube instrumented with 18 thermocouples. The thermocouples are soldered into grooves cut in the relatively thick tube wall. Kapton™ coated strip heaters are wrapped longitudinally along the 8 feet of the test section. The heaters' width is not exactly equal to the circumference of the tube, and so there exists a 0.07" gap between edges of the heater. This gap constitutes an adiabatic region, causing a nonuniform circumferential heat flux. This nonuniformity in the heat flux at the outer perimeter is considered to be negligible due to circumferential heat conduction. The heat flux at the inner surface of the tube is considered uniform.

At the ends of the heated length of the test section pressure taps are soldered around the tube. A 1/16" hole is drilled through the pressure tap into the test section, as shown in Figure 3.6. The pressure taps are connected to the differential pressure transducer with insulated 1/4" O.D. copper lines.

Sight glasses for flow visualization are located at the entrance and exit of the test section, outboard of the pressure taps. The inside diameter of the glass tubes is within 0.004" of the inside diameter of the test section, so perturbations in the flow pattern are minimized. A strobe light flashing on these sight glasses makes visual observation of the flow patterns easier, including such phenomena as wall dryout and foaming. The ends of the test section are connected to the main refrigerant loop by special zero clearance fittings. These fittings allow removal of the test section without disturbing the tubing on either side of the test section. This arrangement permits quick changes to be made in case of damage to the sight glasses or thermocouples, or to change test sections.

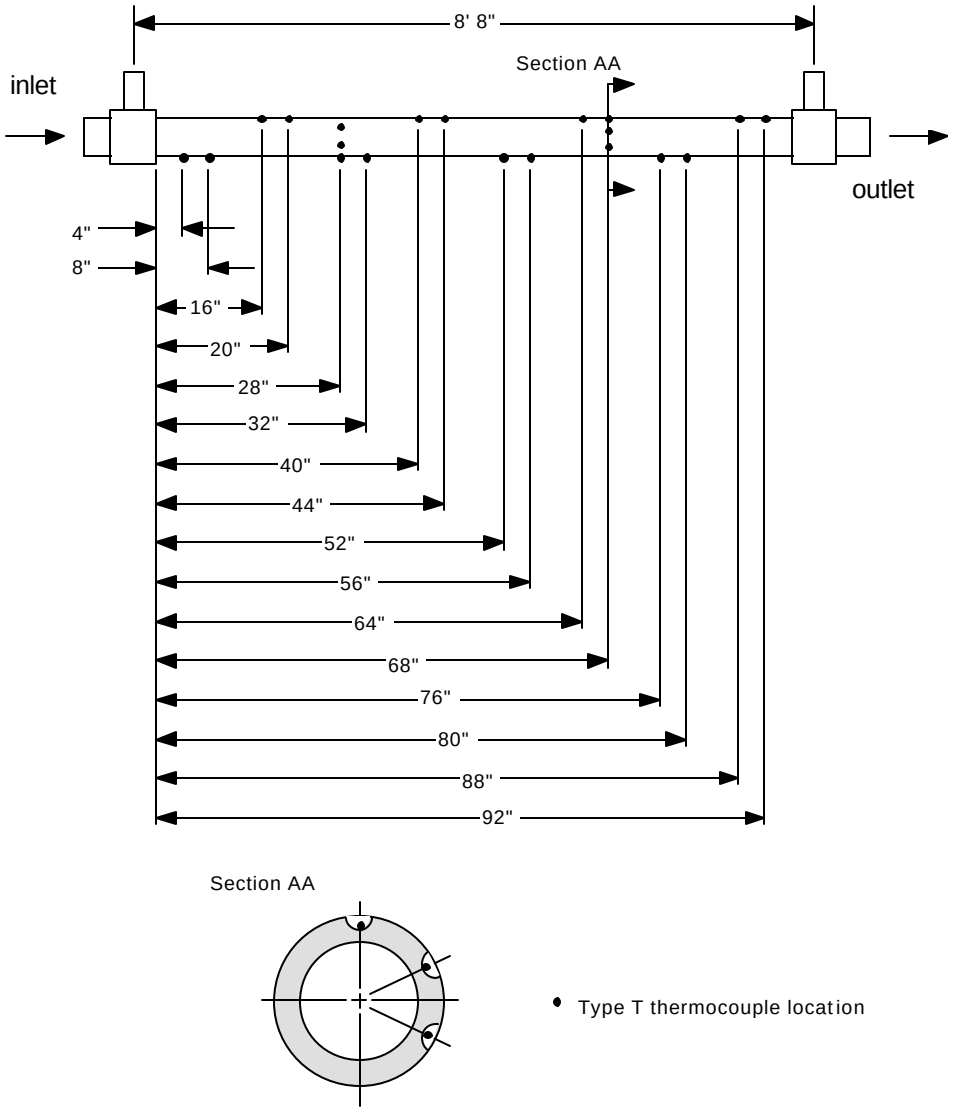

Figure 3.5 Test Section

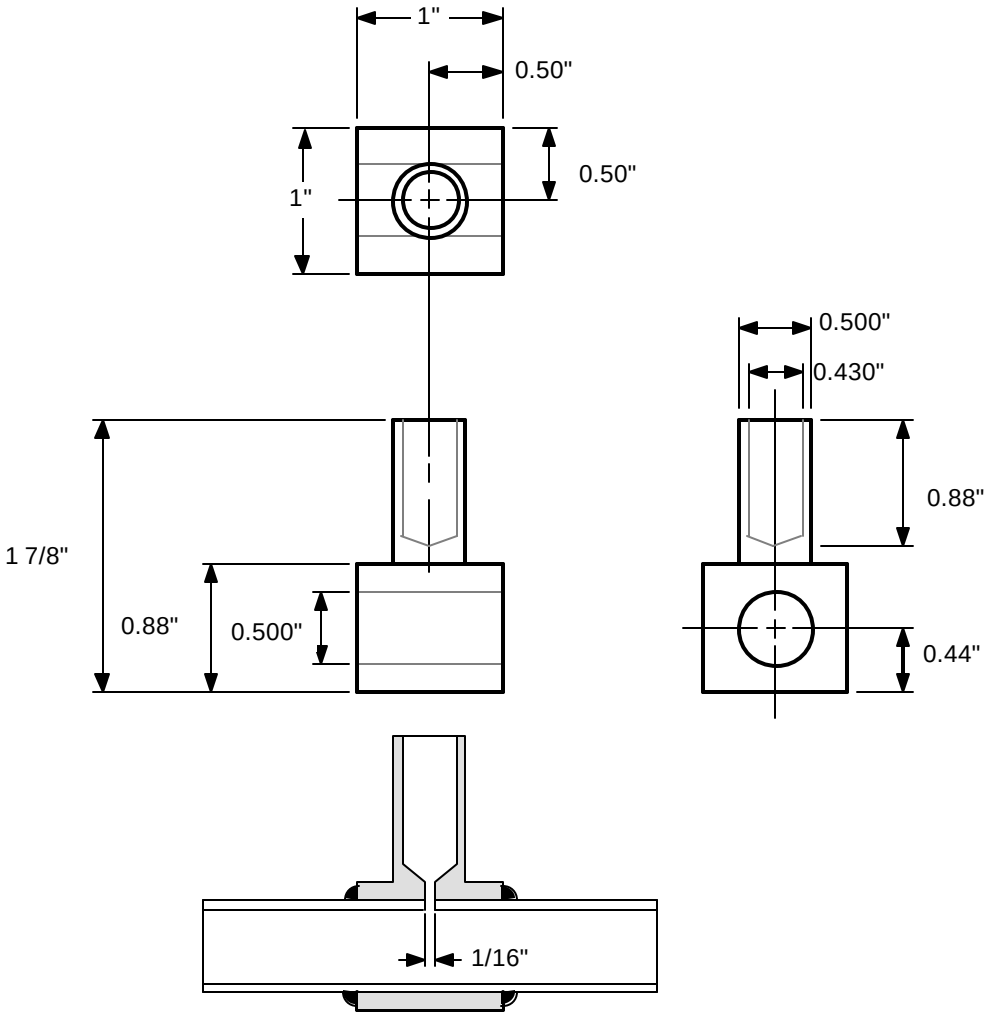

Figure 3.6 Pressure Taps

3.2. Instrumentation

A brief description of instrumentation and controls will be given here. More details can be found in the thesis by Wattelet [1990] and in Wattelet et al. [1990].

3.2.1 Temperature

Three temperatures are measured: refrigerant bulk fluid temperature, test section wall temperature, and brine solution bulk temperature. All temperature measuring devices were calibrated in a controlled temperature bath against NIST-traceable precision mercury thermometers. Uncertainty of temperature measurements after processing in the data acquisition system is considered to be ±0.4°F (±0.2°C).

Refrigerant bulk temperature is measured in five locations with 1/16" diameter probes extending into the center of the tube in which the refrigerant flows. The probes consist of type T copper-constantan thermocouples grounded to a stainless steel outer sheath. Extension wires of the same type for all thermocouples are 30 gauge instrument grade.

Type T thermocouples also measure test section wall temperatures. Wires are 30 gauge instrument grade, and are all from the same original spool of wire. This allows one calibration curve for all thermocouples made from the same alloy on the spool. No extension wires are used in these thermocouples, as junctions are wired directly to the data acquisition system's terminal panels.

Brine solution temperatures are measured by 1/4" probes with an internal platinum resistance temperature detector (RTD). The RTD's used are 100 ohm three wire devices from Omega Company, with the European temperature coefficient of 0.00385 ohms/ohm °C.

3.2.2. Pressure

Refrigerant absolute pressures are measured in three locations: exit of the condenser, inlet of the preheater, and inlet of the test section. In addition, differential pressure is measured across the test section. All four pressure sensing devices are calibrated against a primary standard, the dead weight tester. Uncertainty of the pressure measurement reported by the data acquisition system is considered to be ±0.3% of the full scale reading.

All absolute pressure transducers are BEC company Models GWP5-46AW. The range of the transducer located at the inlet to the preheater is 0-300 psia (0-2050 kPa). The range of the other two absolute pressure transducers is 0-50 psia (0-350 kPa). The differential pressure transducer is a Sensotec Model AD111AT, with a range of 0-5 psid (0-35 kPa). All transducers output 4-20 mA for the given range of measurement.

The absolute pressures are measured through a tap with a 1/16" hole drilled into the tube where the refrigerant flows. These taps are identical to the ones used on the test section for differential pressure measurement, shown in Figure 3.6. Taps are connected to the transducers by 1/4" insulated copper lines.

3.2.3. Heater Electrical Power

Electrical power dissipated by the heaters is measured by watt transducers. A special feature of the transducers is a 10 second averaging time constant. This averaging time allows smoothing of the power peaks caused by SCR (silicon controlled rectifier) switching.

Electrical power is measured in three places: Preheater, test section strip heater bank, and chiller false load heater. All watt transducers are made by Ohio Semitronics, Inc. The preheater and false load heater watt transducers are Models PC5-50B with ranges of 0-34,122 Btu/hr (0-10 kW). The test section heater bank watt transducer is a Model PC5-49B with a range of 0-17,060 Btu/hr (0-5 kW). Output of all three transducers is 0-10 VDC, and uncertainty of the reading is ±0.5% of full scale.

3.2.4. Flow Rate

Refrigerant volumetric flow rate is measured by a Max Machinery Model 214-411 four piston positive displacement flow meter. The flow meter is located after the main refrigerant bypass line, and measures the amount of refrigerant flowing through the preheater and into the test section. The capacity of the flow meter is 0-1 gpm, and the output signal is 0-10 VDC. Uncertainty of the measurement is ±0.5% of full scale reading.

The flow rate of brine solution is measured by a Flow Technology Model FT-16 turbine flow meter. This flow meter is very sensitive to changes in fluid viscosity, and must be calibrated against curves from factory data. The output of this flow meter is a square wave of variable frequency which is proportional to the rotational speed of the turbine. Accuracy is ±1% of full scale reading.

3.2.5. Oil Concentration Measurement

The amount of oil dissolved in the refrigerant is measured with a technique similar to the procedure outlined in ASHRAE Standard 41.4. However, only one sample is taken at the beginning of each series of test runs, instead of the three samples required by the Standard.

The general procedure is to first evacuate and weigh a sampling cylinder, shown in Figure 3.7. Next, a sample of subcooled liquid refrigerant-oil mixture is introduced into the cylinder, and it is weighed again. The difference in mass of these first two readings is the total mass of oil and refrigerant present in the cylinder. Then the refrigerant is slowly boiled away, leaving only oil behind. The cylinder is weighed again, and the difference between this final mass and the previous mass is the total amount of refrigerant that was present in the sampling vessel. The ratio of oil mass to refrigerant mass is the oil concentration on a refrigerant basis, ω_o. The ratio of oil mass to total mass of oil and refrigerant is the oil concentration on a sample basis. All concentrations reported herein use the refrigerant basis.

Many potential sources of error exist in this technique if great care is not taken while sampling. Adding air into the initial sample mass, leaving oil behind in the hose, and not removing all the refrigerant from the container for the final mass are some of these potential errors. A more detailed description of the oil sampling technique is included in Appendix B.

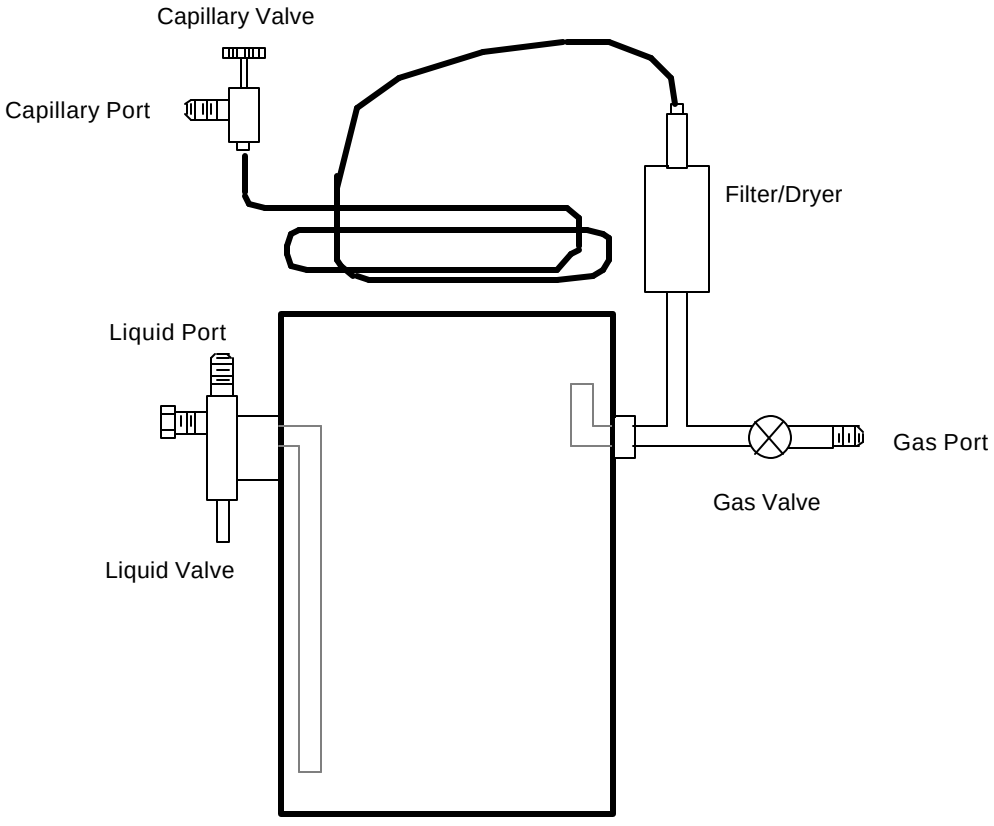

Figure 3.7. Oil Concentration Measurement Sampling Cylinder

3.3. Controls

A total of 6 adjustments can be made for a given test run: 3 heater power levels, pump speed, pump bypass, and refrigerant charge.

3.3.1. Heater Electrical Power Controls

Power dissipated in the heaters is controlled directly from the microcomputer. A control signal is sent out from the computer into the SCR controllers, which act as electronic switches controlling the duty cycle of the heater.

The false load heater SCR is controlled by a 0-10 VDC signal sent out from the computer by the operator. The preheater and test section heater SCR's are controlled by a 4-20 mA signal sent from the computer. The SCR's are slightly nonlinear, and are very sensitive to changes in their internal bias and gain potentiometer settings.

3.3.2. Refrigerant Charge Control

The amount of charge in the test loop has a significant effect on the operating characteristics. If insufficient charge is present, the liquid level in the condensers will fall to the point where there is insufficient subcooling at the pump inlet. Insufficient charge can also reduce the pressure in the test section, which results in a low temperature.

If too much charge is present, the condensers are full of liquid and condensing area is small. This does not allow the brine solution to condense enough flow rate of two-phase mixture. As a result the pressure and temperature of two-phase refrigerant in the test section increases.

The amount of charge in the test loop is controlled by adding or removing refrigerant through the service ports at the exit of the test section or the inlet of the refrigerant pump. When a refrigerant-oil mixture is present in the test loop, it is impossible to add refrigerant without changing the oil concentration. In this case it is desirable to start out with a large amount of charge with the correct oil concentration and remove subcooled liquid refrigerant-oil mixture from the pump inlet as testing proceeds.

Care must be taken by removing charge slowly, as to not interrupt subcooled liquid flow through the pump. This type of transient can quickly result in total loss of refrigerant flow, since the gear pump is designed to only pump liquids.

3.3.3. Flow Rate Control

Controlling refrigerant volumetric flow rate sets the test section mass flux. Adjusting the needle valve in the bypass line around the pump provides coarse control. A potentiometer adjusting pump rotational speed provides much finer control of the mass flux.

Chapter 4: Data Acquisition and Reduction

The data acquisition and reduction system consists of an Apple™ Macintosh™ II microcomputer, Strawberry Tree™ hardware and software, and commercial spreadsheet software. The data acquisition system is capable of accepting up to 48 differential analog inputs, with 12 or 16 bit accuracy. Data retrieved from the loop are displayed by Strawberry Tree's™ WorkBench™ software and logged to a hard disk. Control signals are output to the three different heaters in the test loop. Data reduction software includes spreadsheets for averaging and automatic algebraic manipulation of test data. An estimate of the total experimental uncertainty is also made here.

4.1. Data Acquisition Hardware

The hardware used for data acquisition includes an Apple™ Macintosh™ II microcomputer, four acquisition boards, and six remote terminal panels, shown in Figure 4.1. The acquisition boards plug directly into the motherboard of the computer. The terminal panels are mounted on the test loop framework and are connected to the acquisition boards by ribbon cable. Various sensors are connected to the terminal panels through appropriate wiring.

Three of the acquisition boards have analog input to digital conversion accuracy of 16 bits, while a fourth has accuracy of 12 bits. The accuracy of the analog output channels is 12 bits in all cases. The boards convert the incoming analog voltage to a frequency, which is then counted and timed. Voltage inputs in the 0-50 mV range from type T thermocouples are compared directly to a 100 point temperature lookup table in hardware memory.

The six terminal panels allow a wide variety of sensors to be connected to the microcomputer. Thermocouples, RTD's, voltage inputs, and current inputs are all handled by the T21 and T51 terminal panels. The T21 panels, used primarily for thermocouple measurements, have an isothermal block and precision NIST-traceable cold junction compensation as an integral part of their construction The T51 panels are used for general voltage, current, and resistance measurements. Both types of panels have voltage or current output capability for controlling heater banks remotely from the microcomputer.

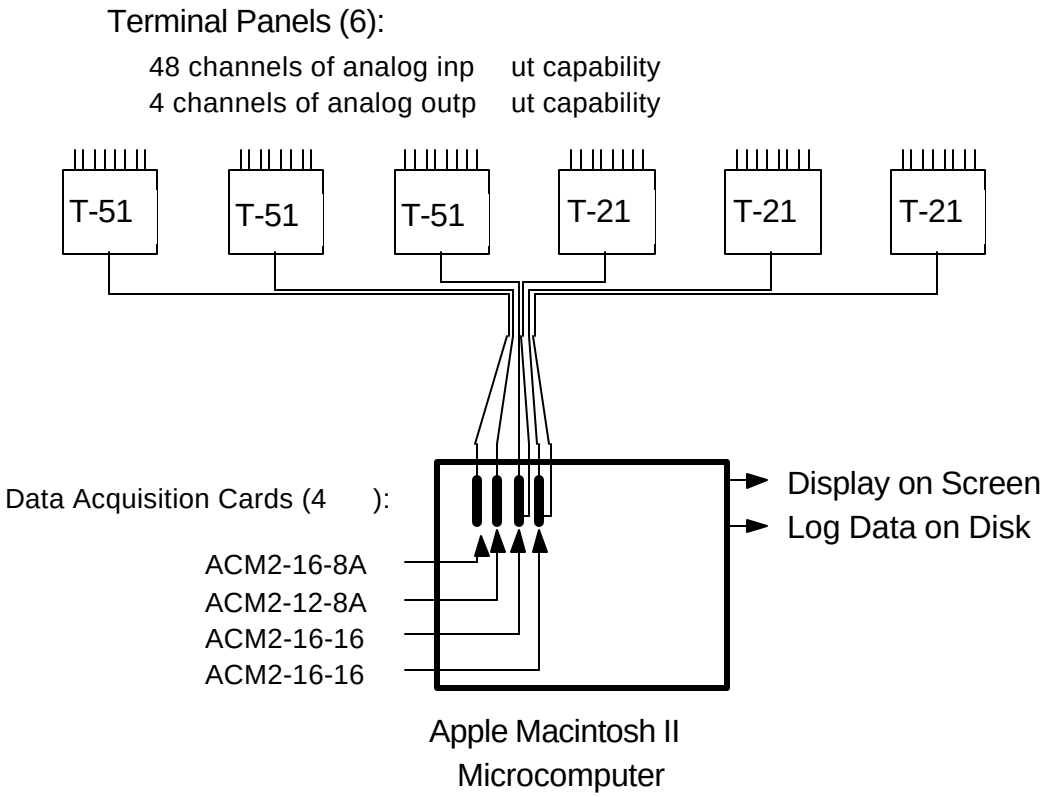

Figure 4.1. Data Acquisition Hardware

4.2. Data Acquisition Software

A program called WorkBench™ by Strawberry Tree™ controls the data acquisition hardware. This program allows the operator to input, manipulate, and display data on the monitor. Data can also be logged to floppy or hard disks. The software is programmed by linking various icons on a worksheet, Figure 4.2. The link sends the output of one icon into the input of another icon.

Analog input icons are set for the proper terminal panel and channel, format (voltage, current, or resistance ranges), resolution, and sampling frequency. All channels for the test runs are sampled at 1 Hz in the noise rejection mode. Maximum resolution for each channel is selected, either 16 or 12 bits. All primary data channels are measured at 16 bit accuracy. Less important control or cross checking inputs are measured at 12 bits resolution.

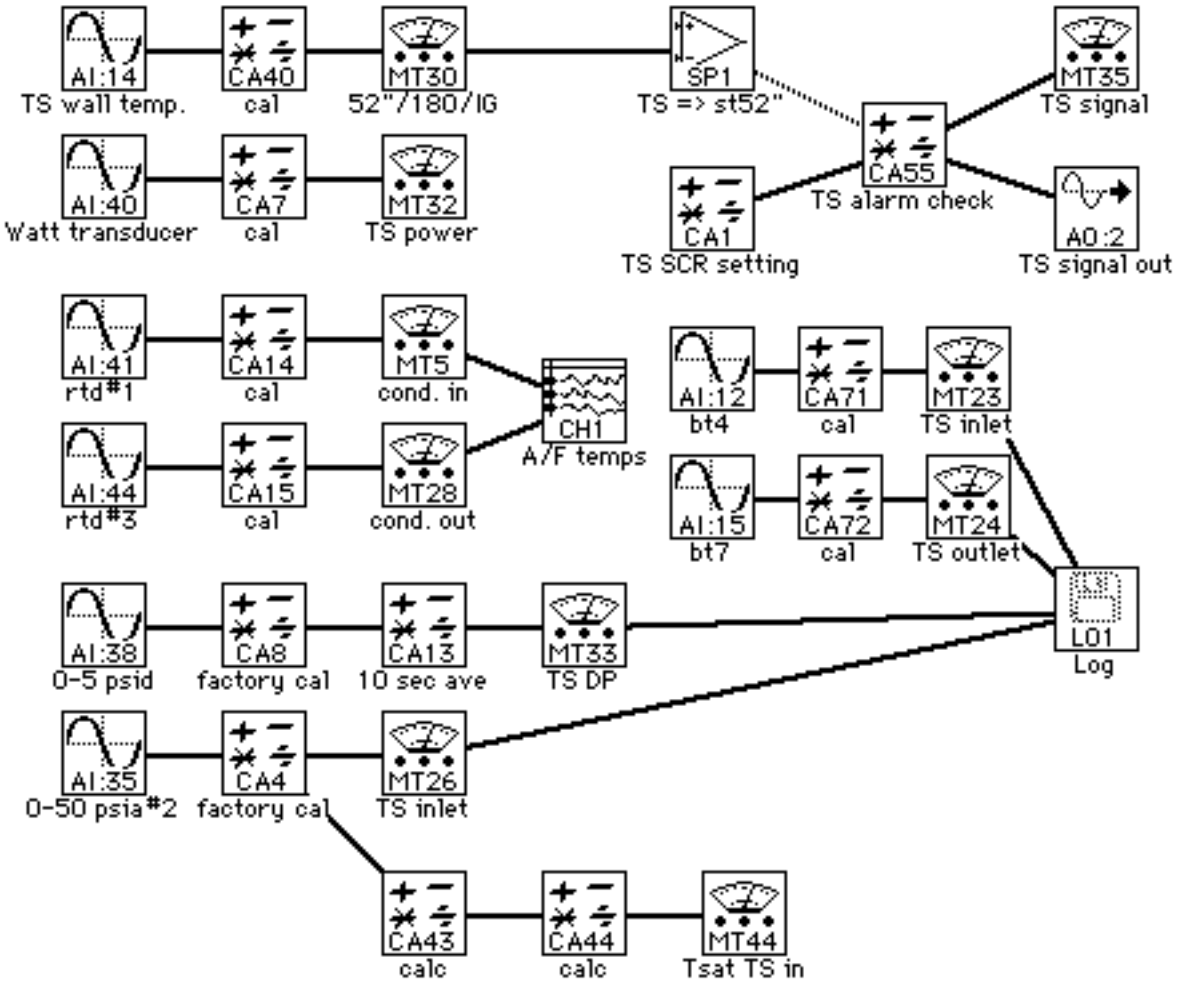

Figure 4.2. Data Acquisition Software Typical Worksheet

Calculation icons perform mathematical calculations on the inputs. This allows scaling of analog inputs to match any calibration curves previously determined or to convert them for display in engineering units. Some inherently turbulent values can be averaged before being linked to meter icons for display. All logged values, however, are "instantaneous" measurements - the averaging is done for on-screen display solely for the operator's benefit. Groups of calculation icons can be strung together to display combinations of variables. For example, the quality of refrigerant at the test section inlet is a combination of the refrigerant mass flow rate, preheater power, and temperature and pressure at the inlet and outlet of the preheater. A particularly useful application of the calculation icons is to determine refrigerant properties as a function of measured temperature or pressure, based on curve fits of ASHRAE data. Heat of vaporization, saturation temperature, density of refrigerant - oil mixture, and refrigerant liquid enthalpy are only some of the thermophysical properties calculated online. Other information includes the amo unt of subcooling at the preheater and pump inlets and mass flux in the test section.

Meter icons display calculated values in any desired units or amount of significant figures.

Graph icons allow variables to be displayed versus time. This is particularly helpful in determining if a steady state condition has been achieved in the test loop. Identification of undesirable transient conditions is possible by observing a given temperature versus time on a graph window.

Analog output icons are set by the operator to control the signal given to the SCR switches. This allows remote control of the power level in any of the three heaters.

Alarm icons compare some input to a setpoint and output a true or false condition. Inputs to these icons are usually temperatures or pressures, and they are used to automatically turn off heater banks if a dangerous condition is detected.

Log icons allow the operator to write data to a hard or floppy disk. The format of the logged data can be adapted to various standards, allowing easy manipulation by standard commercial spreadsheets or word processors. In this research, logging frequency was once per second for 60 or more seconds. If a low frequency steady oscillation existed at the test condition, logging time was increased to cover at least 10 full oscillations.

4.3. Data Reduction Techniques

The WorkBench™ software allows on-line calculation of quality entering the test section and mass flux in the test section. Quality is defined as:

$$x_{ts,in} = \frac{i_{(ts,in)} - i_l}{i_{fg}} \tag{4.1.}$$

where $i_{(ts,in)}$ is the refrigerant enthalpy at the test section inlet, i_l is the enthalpy of saturated liquid based on the pressure of the test section inlet, and i_{fg} is the enthalpy of vaporization based on the pressure of the test section inlet. If one assumes that refrigerant entering the preheater is subcooled, then $i_{(ts,in)}$ can be assumed to be the enthalpy of saturated liquid at the temperature entering the preheater plus the amount of heat added in the preheater per unit mass flow rate in the test section:

$$i_{(ts,in)} = i_{l(ph,in)} + \frac{\dot{q}_{ph}}{\dot{m}_{ts}} \tag{4.2.}$$

This procedure is calculated online by the WorkBench™ software. Curve fits calculate the required enthalpies based on temperature or pressure. A typical block of calculations for finding quality is shown in the WorkBench™ quality worksheet, Figure 4.3.

Mass flux in the test section is also calculated on-line. Curve fits of liquid refrigerant and oil densities are based on the mixture temperature at the flow meter. The density of the mixture at the flow meter is calculated by the following relation:

$$\frac{1}{\rho_{mix}} = \frac{1 - \omega_o}{\rho_{ref}} + \frac{\omega_o}{\rho_o} \tag{4.3.}$$

Mass flux is then the product of volumetric flow rate measured by the flow meter and mixture density divided by cross-sectional area of the test section tube. On-line calculation of mass flux in the test section is shown in a WorkBench™ mass flux worksheet, Figure 4.4.

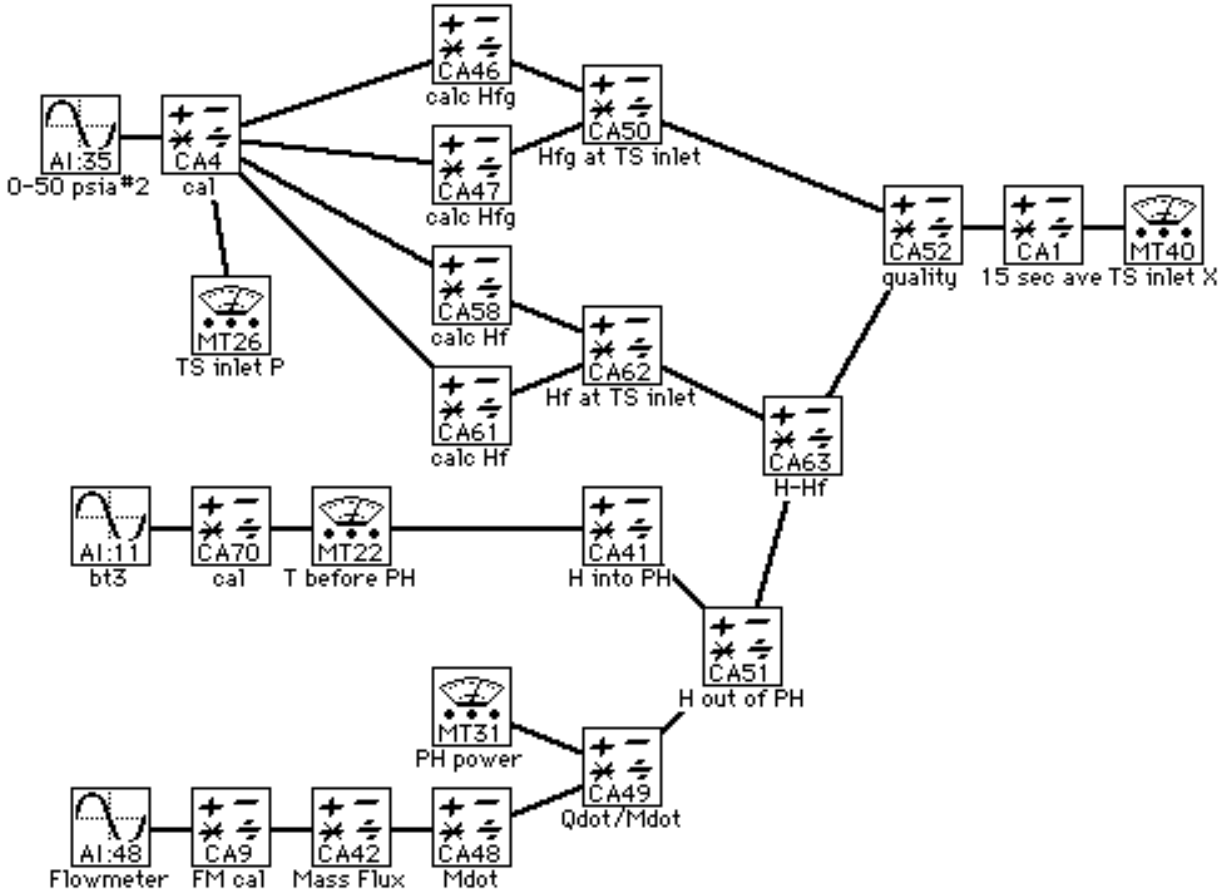

Figure 4.3. Quality Worksheet

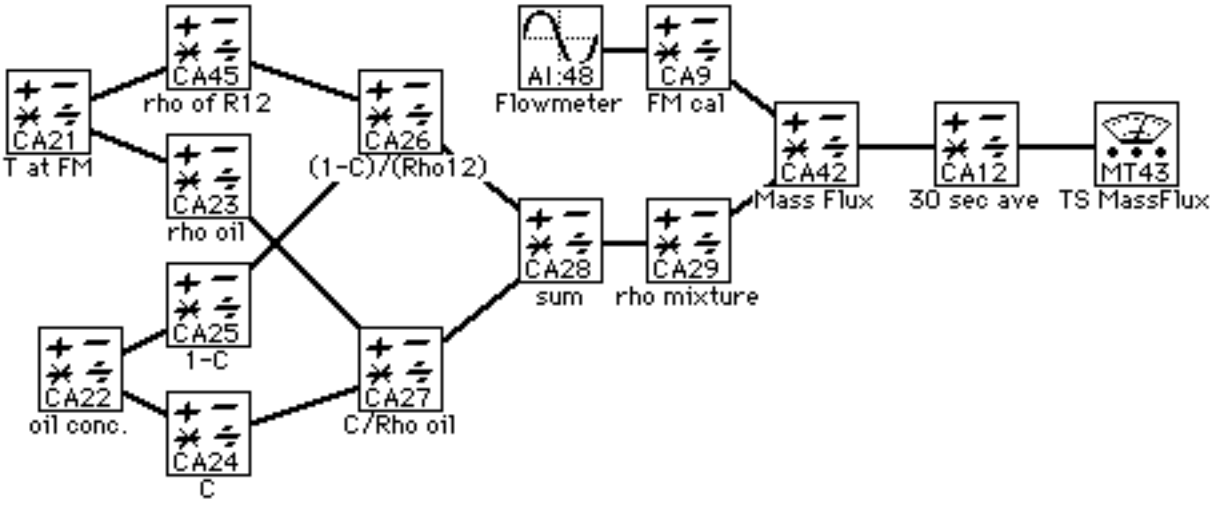

Figure 4.4. Mass Flux Worksheet

4.4. Data Reduction Software

Once the data is logged by WorkBench™, it is read into Microsoft Excel™ spreadsheets which average the values collected over time. The spreadsheet calculates the heat transfer coefficient (h), defined as:

$$h_{tp} = \frac{\phi_{ts}}{T_{wall}-T_b} \qquad (4.4.)$$

where ϕ_{ts} is simply the measured power input to the test section divided by the inside wall area of the test section tube, T_{wall} is a weighted average of thermocouple wall temperatures, and T_b is the average of thermocouple measurements of bulk fluid temperatures at the test section inlet and outlet. T_{wall} is defined as:

$$T_{wall} = 0.25\, T_{top} + 0.25\, T_{bottom} + 0.50\, T_{side} \qquad (4.5.)$$

where T_{top} is the average temperature of top wall thermocouples, T_{bottom} is the average temperature of bottom wall thermocouples, and T_{side} is the average temperature of side wall thermocouples.

Once the sensor readings are averaged and h is calculated, the first Excel™ spreadsheet passes on linked values to the second Excel™ spreadsheet. This second spreadsheet is known as a 'ledger sheet' since it is kept in a binder or ledger as a hard copy of the experimental results. An example of a ledger sheet is given in Figure 4.5.

Single Tube Evaporator Two Phase Test

Run #: 1
Date: 9/23/91
Test Section: #2
Refrigerant: HFC-134a
Data Disk: 23

Surface Temperatures (°C):

4"/180/IG	7.5
8"/180/IG	7.3
20"/0/UH	9.0
28"/180/UH	8.8
28"/120/UH	8.2
28"/60/UH	7.6
32"/180/UH	8.3
40"/0/IG	7.5
44"/0/IG	7.5
52"/180/IG	7.5
56"/180/IG	7.3
64"/0/UH	8.1
68"/0/UH	8.0
68"/60/UH	8.3
68"/120/UH	7.9
80"/180/UH	8.0
88"/0/IG	6.9
92"/0/IG	6.8

Mass Flux (kg/s-m^2):	301	
Heat Flux (kW/m^2):	10.1	
Inlet quality:	19.8%	dx: 16.7%
Inlet Sat. Temp.:	5.1°C	
Oil Concentration:	1.0%	
Oil Type:	PAG 0354	

	temp. (°C)	press. (kPa)
before rcvr:	-0.6	312.5
after pump:	0.4	N/A
before PH:	0.9	350.6
TS inlet:	5.1	343.7
TS outlet:	4.9	339.9
HX inlet:	-1.5	N/A
HX outlet:	-0.6	N/A
after FLH:	0.9	N/A

	power (kW)	SCR settings	
Test Section:	0.79	5.9	mA
Preheater:	1.07	5.9	mA
FLH:	5.09	5.0	VDC

	h (w/m^2-K)
overall:	3449
first half of TS:	3425
second half of TS:	3474

Test Section dP: 3.8 kPa

Operator: Adriano
Inlet Flow Pattern: wavy annular
Outlet Flow Pattern: wavy annular
TXV: low
Comments: foaming is not observed, and an annular film is observed on top of the sight-glass

Figure 4.5. Ledger Sheet

Chapter 5: Discussion of Results

The tests run during this research are discussed here. Two refrigerants were investigated, CFC-12 and HFC-134a. Three different oils were studied in the HFC-134a tests: PAG 0332, PAG 0354, and Ester 0540. The temperature at the inlet to the test section for each run was 5°C. The specific test conditions and raw data obtained are detailed in Appendix C. This chapter will discuss the uncertainty analysis and the various trends in heat transfer coefficients and pressure drops observed in both pure refrigerants and refrigerant-oil mixtures.

5.1. Uncertainty of Results

An uncertainty analysis should be performed in any experimental investigation so that instrumentation which has the largest impact on the uncertainty can then be identified and refined.

The variables which affect uncertainty of the heat transfer coefficient measurement are all in the test section: heater power, internal surface area, wall temperature, and bulk refrigerant temperature. Test section pressure drop uncertainty is calculated from the gauge's accuracy. In addition, errors introduced by the data acquisition system must be considered.

The method of uncertainty calculation used is that of sequential perturbation described by Moffat (1988). The experimental uncertainty of the heat transfer coefficient measurements ranges from 3.7% to 15.3%. The experimental uncertainty of the pressure drop across the test section is 0.6%.

Additional insight into the uncertainty of the results can be seen by the repeatability of the trials. Nearly identical test conditions were run by different operators and at different times. The results in both heat transfer coefficient and pressure drop were within 5%. Examples of this repeatability can be seen in Appendix C, where similar test conditions show sometimes nearly identical results.

5.2. Pure Refrigerant Heat Transfer

The parameters varied in this investigation include quality, mass flux, and heat flux. Most of the tests run had stratified or annular flow patterns. A phenomenon known as dryout occurred for some tests with relatively high qualities, when the annular liquid film on the wall began to completely evaporate. This was detected both by visual observation and a sudden decrease in heat transfer coefficient due to a rise in wall temperature. Note that the thermodynamic quality at this condition can still be less than unity, as droplets of liquid are still suspended in the vapor core. In horizontal tubes with a uniform heat flux, dryout first occurs in the top region of the tube where liquid layer is thinner. This was also confirmed by visual observation.

The effect of the average test section quality (x_{ave}) can be seen in Figures 5.1. and 5.2. In general, h_{tp} increases with increasing average quality in the annular flow regime. Intense evaporation at the liquid-vapor interface decreases the liquid film thickness, presenting a smaller thermal resistance to the convective boiling heat transfer dominant in the annular flow regime. There is no major effect of quality on circumferentially averaged heat transfer coefficients in the stratified flow regime, G = 100 kg/m^2-s. In this flow regime, top heat transfer coefficients were lower than bottom coefficients due to the wetting of the bottom surface only.

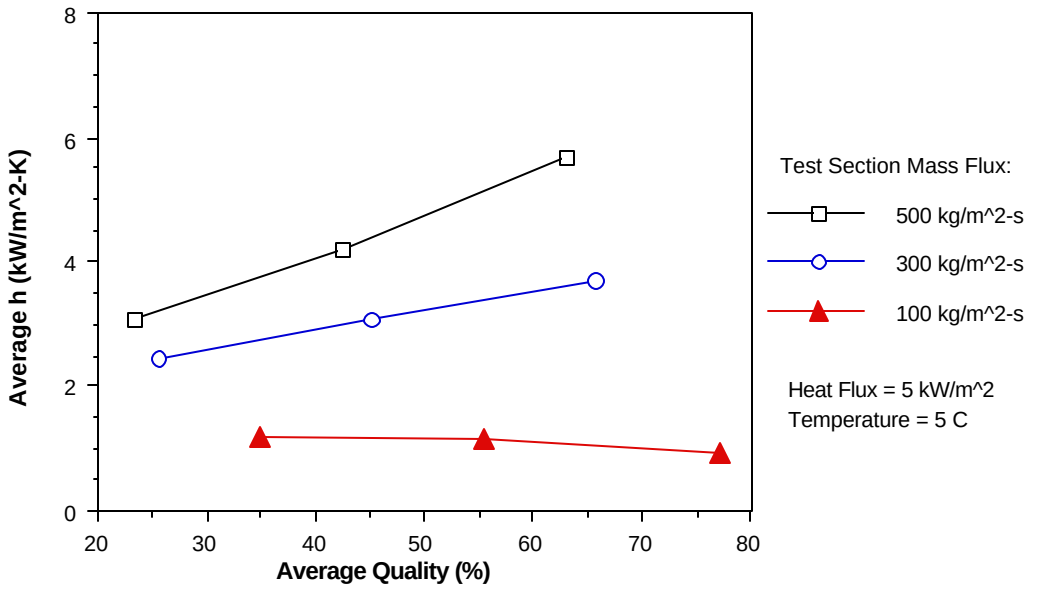

Figure 5.1. Pure CFC-12, Average h vs. Average Quality at Constant Heat Flux

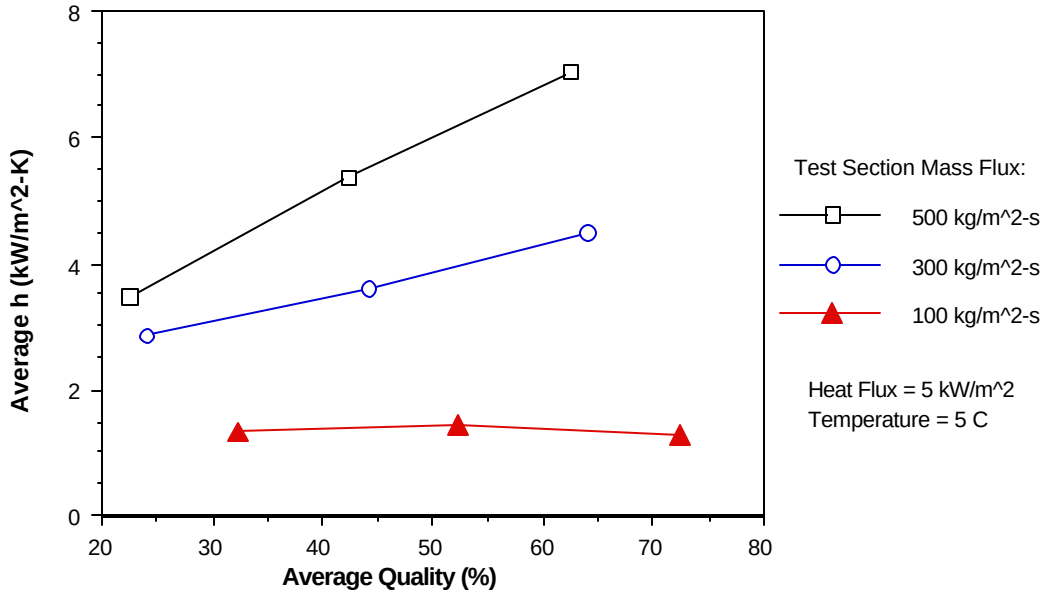

Figure 5.2. Pure HFC-134a, Average h vs. Average Quality at Constant Heat Flux

The effect of mass flux (G) on heat transfer coefficient can also be seen in Figures 5.1. and 5.2. As mass flux is increased, h_{tp} increases. The increase in h_{tp} is due to both higher liquid velocities and to a transition of flow regimes. At low mass fluxes (G=100 kg/m^2-s), the flow regime is stratified flow, with only the bottom part of the wall area wetted by refrigerant. As G increases, the flow regime changes to an annular pattern. The liquid portion completely wets the wall, and a vapor core flows in the center of the tube. Heat transfer coefficients are typically much higher in the annular regime than in the stratified regime.

Varying the heat flux (ϕ) in the test section does not seem to affect the heat transfer coefficient significantly, as shown in Figures 5.3. and 5.4. At the qualities tested, convective boiling is the dominant mode of heat transfer. Nucleate boiling, which is strongly affected by heat flux, is suppressed at these qualities and mass fluxes.

Comparing Figure 5.1. with Figure 5.2. and Figure 5.3. with Figure 5.4. also shows that, in general, HFC-134a has a higher h_{tp} than CFC-12 at identical conditions. This can be explained in part by the fact that HFC-134a has a higher liquid thermal conductivity than CFC-12.

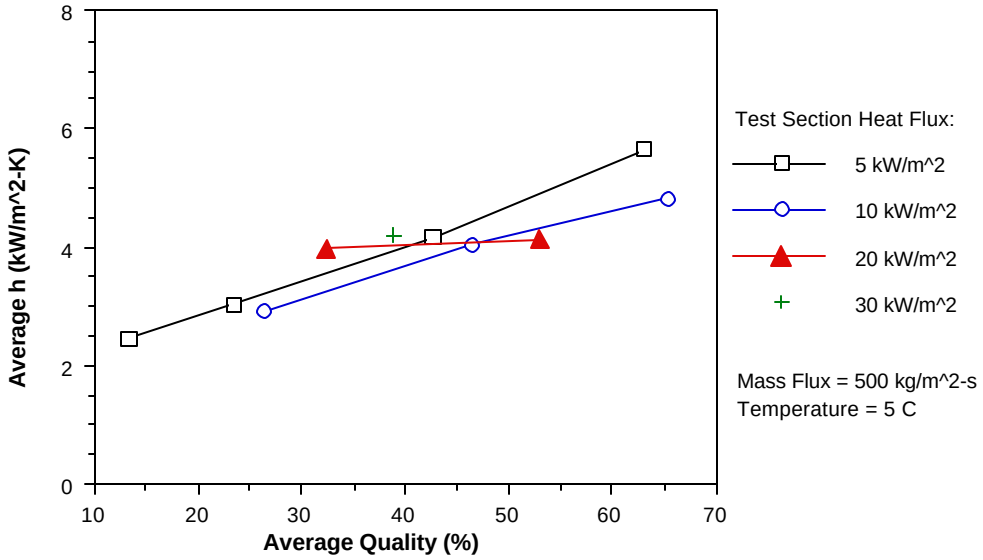

Figure 5.3. Pure CFC-12, Average h vs. Average Quality at Constant Mass Flux

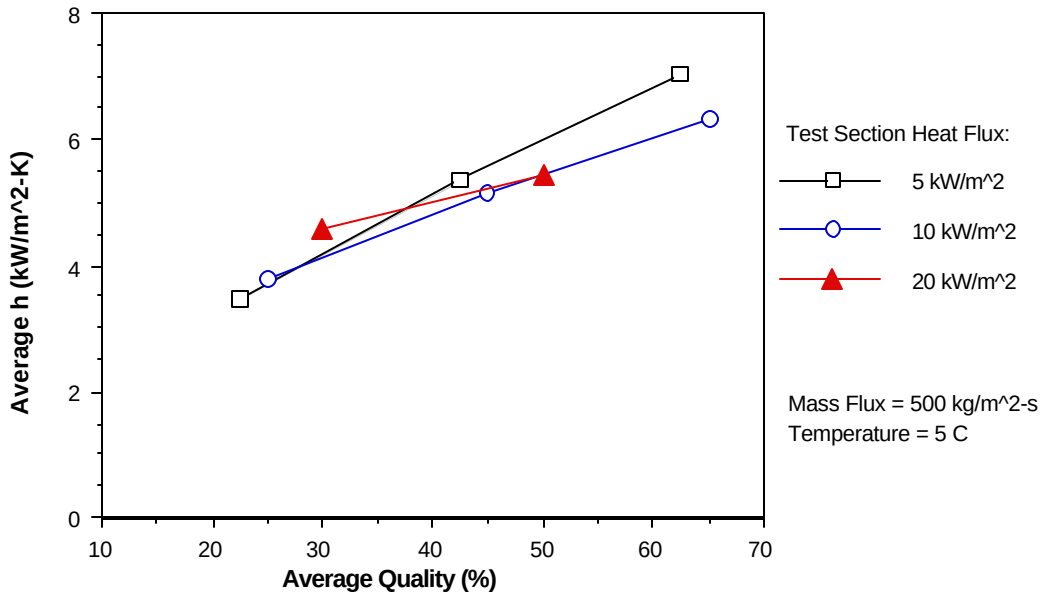

Figure 5.4. Pure HFC-134a, Average h vs. Average Quality at Constant Mass Flux

5.3. Pure Refrigerant Pressure Drop

Pressure drop in pure refrigerant two-phase flow is largely a function of mass flux, average quality, and corresponding flow regime. As is the case for heat transfer coefficient, pressure drops are not strong functions of the test section heat flux. The effects of mass flux and average quality on pressure drop can be seen in Figures 5.5. and 5.6. The pressure drop tends to increase with increasing mass flux and increasing average quality in the annular flow regime, because of the higher overall velocity and higher velocity gradients near the wall surface. Pressure drop is not a strong function of average quality in the stratified flow regime.

Comparing Figure 5.5. with Figure 5.6. shows that, in general, HFC-134a had a higher pressure drop than CFC-12 for similar test conditions. This can be explained by the fact that the liquid kinematic viscosity is 18.5% higher for HFC-134a than CFC-12 at 5°C, as well as the different flow geometries that may exist at otherwise identical conditions.

5.4. Oil Effects on Heat Transfer

Adding oil to a refrigerant changes the properties of the mixture. In general, thermal conductivity may either increase or decrease, while surface tension and viscosity increase. This can affect evaporative heat transfer in several ways. Since thermal conductivity may change, more or less heat may be conducted from the wall through the liquid film. This effect can be difficult to detect, however, unless a high concentration of oil is present.

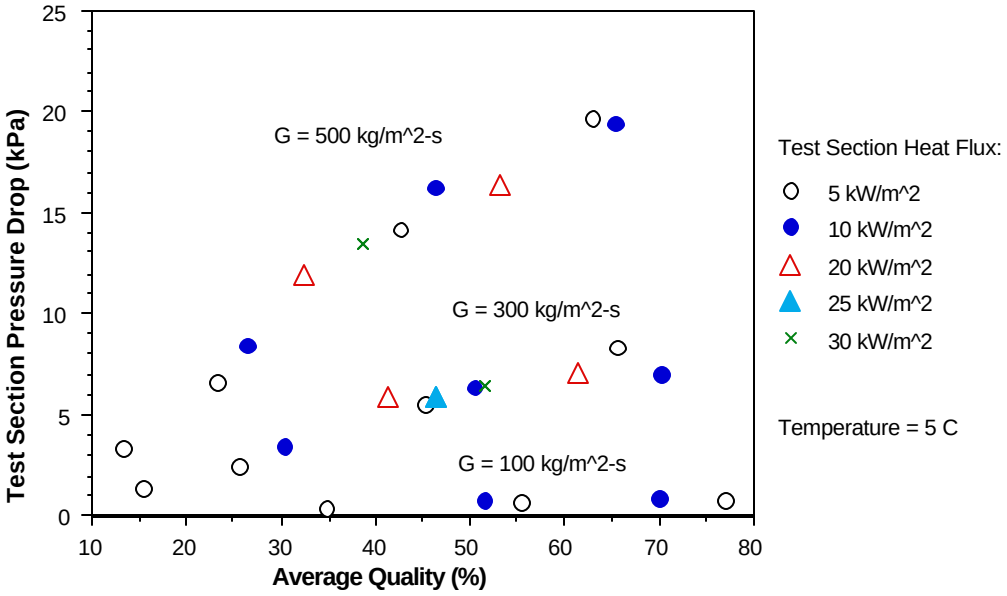

Figure 5.5. Pure CFC-12, Pressure Drop vs. Average Quality

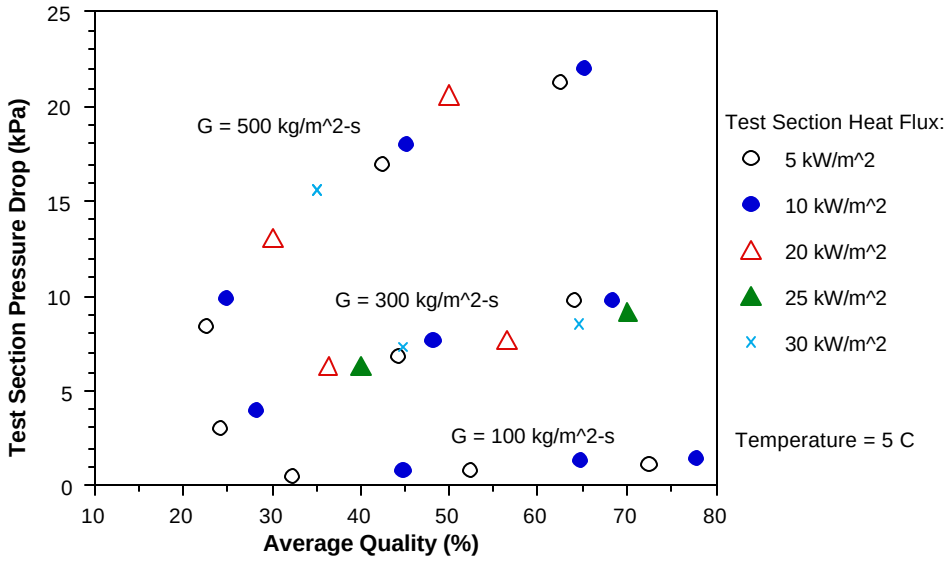

Figure 5.6. Pure HFC-134a Pressure Drop vs. Average Quality

Increasing surface tension will tend to promote greater circumferential wall wetting and higher heat transfer coefficients when the flow pattern is stratified or in transition between stratified and annular. This effect generally increases heat transfer coefficients in the lower quality ranges where the transition occurs. Increasing surface tension will also affect bubble growth after nucleation, but this effect is negligible in these test conditions since nucleate boiling is suppressed.

As quality increases, the uniform liquid phase evaporates refrigerant and contains a higher concentration of oil. Eventually the oil concentration becomes large enough that separation of phases may occur in the liquid layer, depending on miscibility limits. The uniform refrigerant-oil liquid phase separates into two distinct liquid phases, a refrigerant-rich phase and an oil-rich phase. The refrigerant-rich phase still contains some oil, and the oil-rich phase still contains some refrigerant. In the horizontal flow tests run in this research, it has been generally observed that when separation of the liquid phases occurs, the oil-rich phase coats the top of the tube, while the refrigerant-rich phase flows in the lower portion of the tube. This effect can increase heat transfer coefficients in the high quality regions where dryout of the tube wall would occur when oil is not present. An oil-rich phase cools the wall because refrigerant still evaporates from it and heat is conducted from the wall through a liquid oil film (instead of only vapor refrigerant in the absence of oil) . The observed effect is that in refrigerant-oil mixtures, wall dryout occurs at higher qualities.

An additional effect of oil on heat transfer is that of foaming. Foaming occurs in the annular flow regime when the high velocity vapor core agitates the liquid surface enough to promote bubble formation. These bubbles do not immediately collapse because the surface tension of the mixture is higher than that of the pure refrigerant. The bubbles then disperse throughout the liquid layer. This can increase heat transfer between the wall and refrigerant mixture in several ways. The interface between liquid and vapor has a much higher surface area when foaming is present. Bubbles of cool vapor are carried closer to the hot wall, which may result in a faster evaporation rate.

Some of these effects can be seen in Figure 5.7 and 5.8., where an enhancement ratio is plotted as a function of oil concentrations.

This enhancement ratio is simply h_{tp} when the oil is mixed with the refrigerant divided by h_{tp} when refrigerant flows alone at otherwise identical conditions. By definition, the enhancement ratio is one when the oil concentration is zero. Figure 5.7. shows the general trend of enhancement ratios greater than one for lower concentrations of oil and enhancement ratios less than one for high concentrations of oil. At the low mass flux of G = 100 kg/m2-s, the enhancement ratios are greater and persist to higher oil concentrations than at the higher flow rates. This effect is caused by the greater wetting of the top portion of the horizontal tube in stratified flow if oil is present. Figure 5.8. shows that the three different types of oils do not exhibit very different enhancement ratios at otherwise identical conditions.

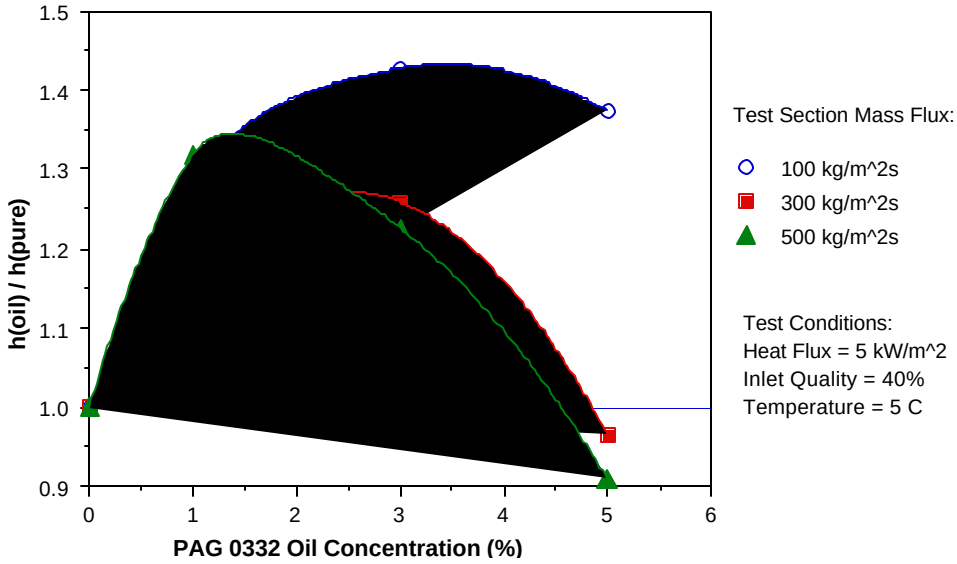

Figure 5.7. HFC-134a/PAG 0332 Mixture Enhancement Ratio vs. Oil Concentration

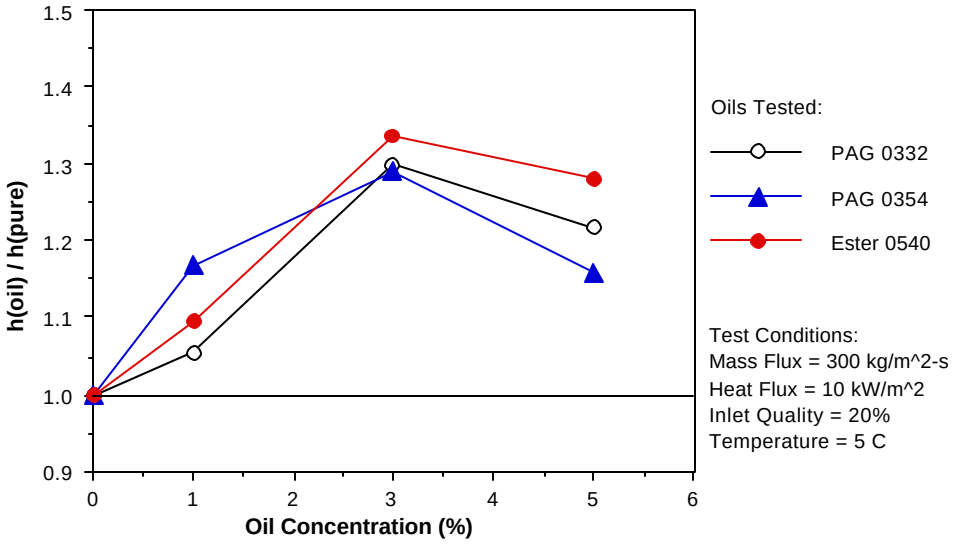

Figure 5.8. HFC-134a/Oil Mixtures Enhancement Ratio vs. Oil Concentration

5.5. Oil Effects on Pressure Drop

The addition of oil to a refrigerant generally increases the viscosity of the mixture. This will tend to increase the pressure drop because of greater shear stresses between the wall and liquid film as well as between the liquid film and vapor core. Figure 5.9. shows the effect of oil concentration on pressure drops at various mass fluxes. Figure 5.10. shows the negligible difference in pressure drops at equivalent concentrations of the three types of oils tested. This is due to the fact that all three oils had similar viscosities at the evaporation temperature of 5°C.

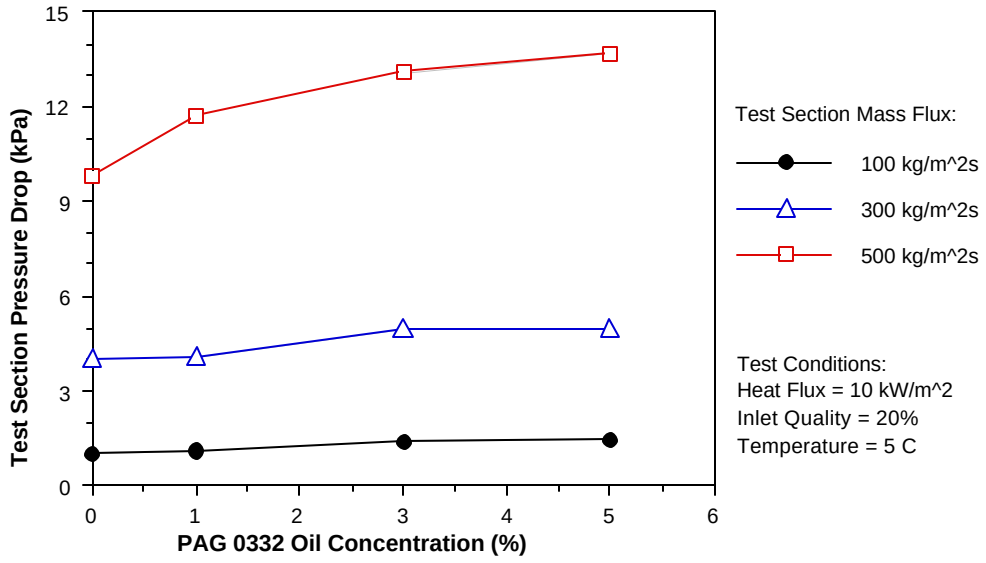

Figure 5.9. HFC-134a/PAG 0332 Mixture Pressure Drop vs. Oil Concentration

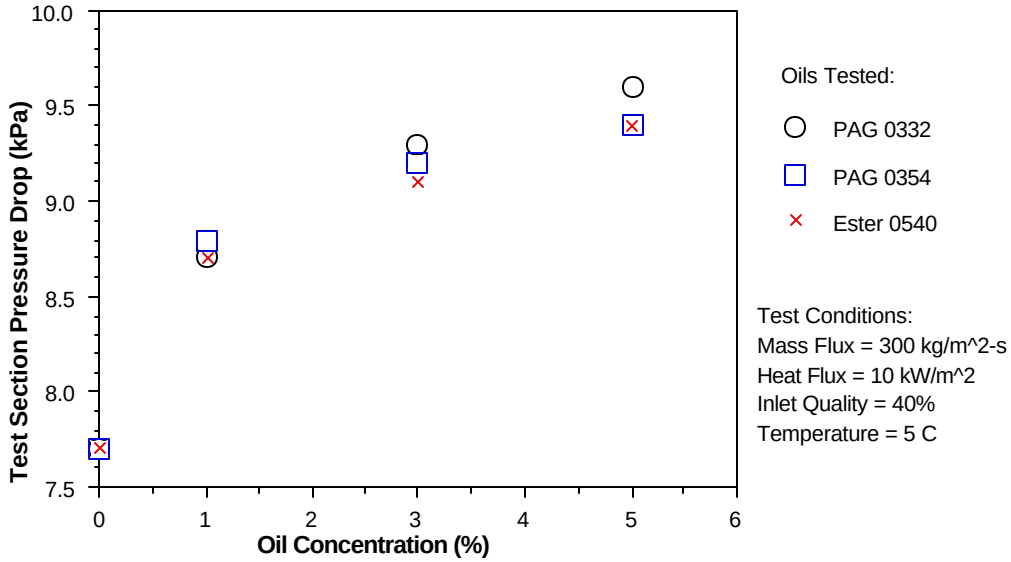

Figure 5.10. HFC-134a/Oil Mixtures Pressure Drop vs. Oil Concentration

Chapter 6: Correlation of Results

The heat transfer results obtained in this research are compared with three correlations in the open literature commonly used to predict evaporative heat transfer coefficients for refrigerants. All three correlations can be applied to turbulent, two-phase, pure refrigerant evaporating in a horizontal, circular, and smooth tube with a constant heat flux wall boundary condition. The three correlations were proposed by Chaddock and Noerager (1966), Kandlikar (1987), and Jung et al. (1989). Mean deviations of the data from each correlation are calculated, and a graph containing the data points and the correlation curve is plotted. Finally, a new correlation is proposed based only on the data gathered during this research.

Correlations for refrigerant pressure drop are widely available in the open literature. New correlations for pressure drop in ozone-safe refrigerants and refrigerant-oil mixtures are not attempted in this work.

6.1. Previous Heat Transfer Correlations

Chaddock and Noerager (1966) proposed a correlation for horizontal two-phase CFC-12 evaporation based on 20 experimental runs. The correlation is of the form:

$$\frac{h_{tp}}{h_{lo}} = \frac{3.0}{(\chi_{tt})^{2/3}} \qquad (2.2)$$

and

$$\frac{h_{tp}}{h_{l}} = \frac{3.0}{\chi_{tt}} \qquad (2.3)$$

The correlations for h_{tp}/h_l and h_{tp}/h_{lo} are shown in Figures 6.1. and 6.2. with our experimental data superimposed. Since the Chaddock-Noerager correlation was based on low inlet quality and therefore high Lockhart-Martinelli parameter data ($x_{in,ts} = 0.20$ and $\chi_{tt,ave} > 0.165$), the experimental data plotted only represent runs where the flow pattern at the outlet of the test section was annular or wavy-annular. Those runs where dryout occurred are not included on the plots. The calculated mean deviation h_{tp}/h_l is 29.7% for CFC-12 and 32.9% for HFC-134a. The calculated mean deviation for h_{tp}/h_{lo} is 27.2% for CFC-12 and 28.1% for HFC-134a. Figure 6.1. also shows our proposed correlation, discussed in section 6.2.

It is interesting to note that the Chaddock-Noerager correlation consistently overpredicts the values of heat transfer coefficient ratios. This may be due to the fact that a small amount of oil used for compressor lubrication was present in their test apparatus. They estimate it to be 0.1% but do not give the method by which this number was calculated. Small quantities of oil can greatly influence flow patterns and heat transfer characteristics.

Kandlikar (1976) proposed a correlation of the form:

$$\frac{h_{tp}}{h_{l}} = c_1 \, Co^{c2} + c_3 \, Bo^{c4} \, F_{fl} \qquad (2.4)$$

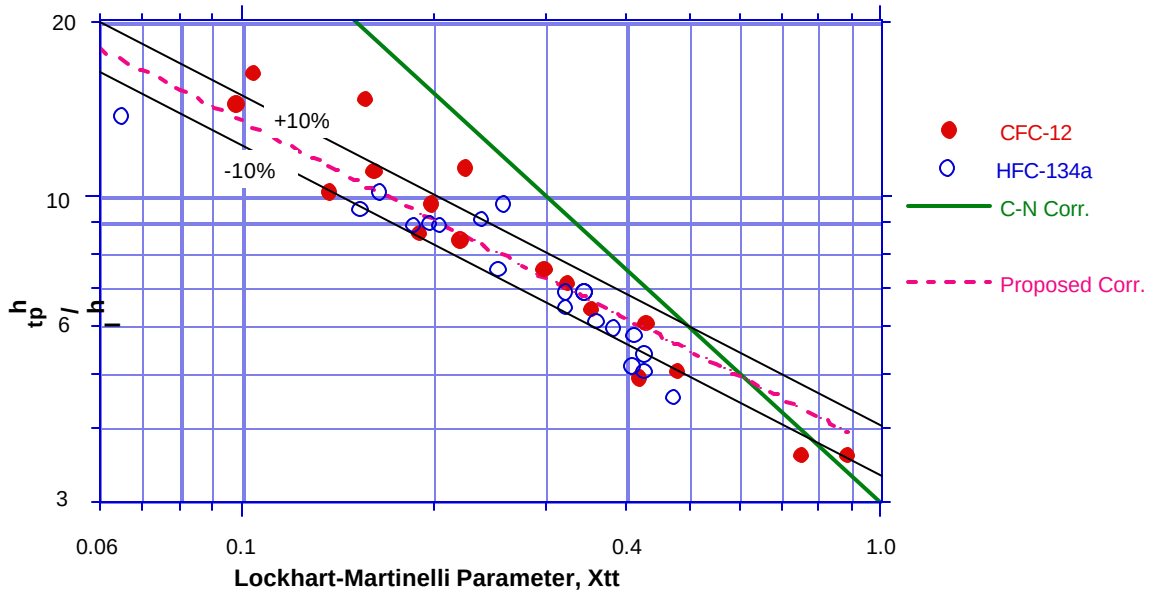

Figure 6.1. Chaddock-Noerager and Proposed Correlations for h_{tp}/h_l vs. experimental annular flow data

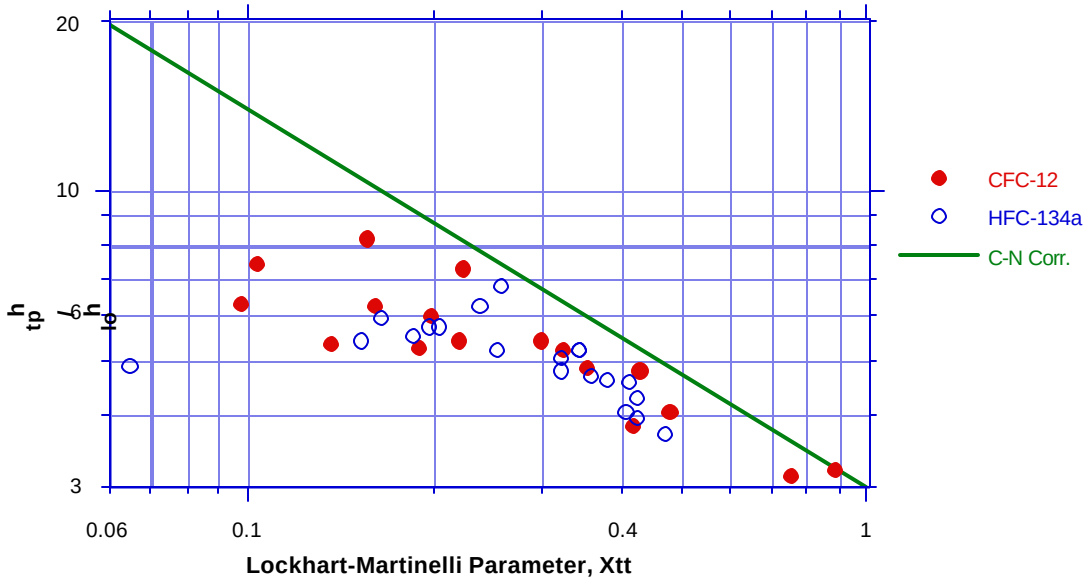

Figure 6.2. Chaddock-Noerager Correlation for h_{tp}/h_{lo} vs. annular experimental data

This correlation was based on over 5000 data points from many different researchers investigating different fluids. A value of F_{fl} of 1.63 for HFC-134a was used, as suggested by Eckels and Pate (1990). The experimental heat transfer coefficient ratios versus the ones predicted by Kandlikar are shown in Figure 6.3. All of the present data is included for this comparison, as the Kandlikar correlation was based on average qualities where all the normal two-phase flow patterns exist. The overall mean deviation of the experimental data from the predicted values is 16.5% for CFC-12 and 16.1% for HFC-134a. This is under the 18.8% mean deviation Kandlikar calculated for all refrigerants in his data set. However, the mean deviation for tests where dryout was observed is 23.0% for CFC-12 and 22.3% for

HFC-134a. Where wavy-annular or completely annular flow was observed, the mean deviations are 11.9% for CFC-12 and 8.3% for HFC-134a.

Jung et al. (1989) proposed a correlation of the form:

$$h_{tp} = N\, h_{sa} + F_p\, h_l \qquad (2.5)$$

This correlation was developed specifically for pure refrigerants and their mixtures. The experimental data is plotted against the values predicted by the Jung et al. correlation in Figure 6.4. The mean overall deviation was 15.8% for CFC-12 and 19.1% for HFC-134a. The mean deviation for runs where dryout was observed is 23.6% for CFC-12 and 26.6% for HFC-134a. The mean deviation for tests where dryout was not observed is 9.5% for CFC-12 and 9.7% for HFC-134a.

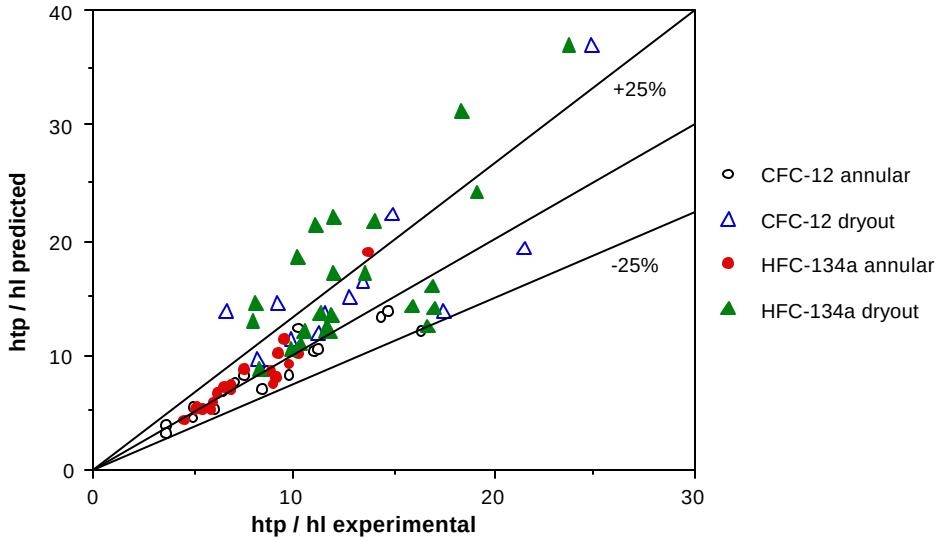

Figure 6.3. htp/hl predicted by Kandlikar Correlation vs. htp/hl experimental

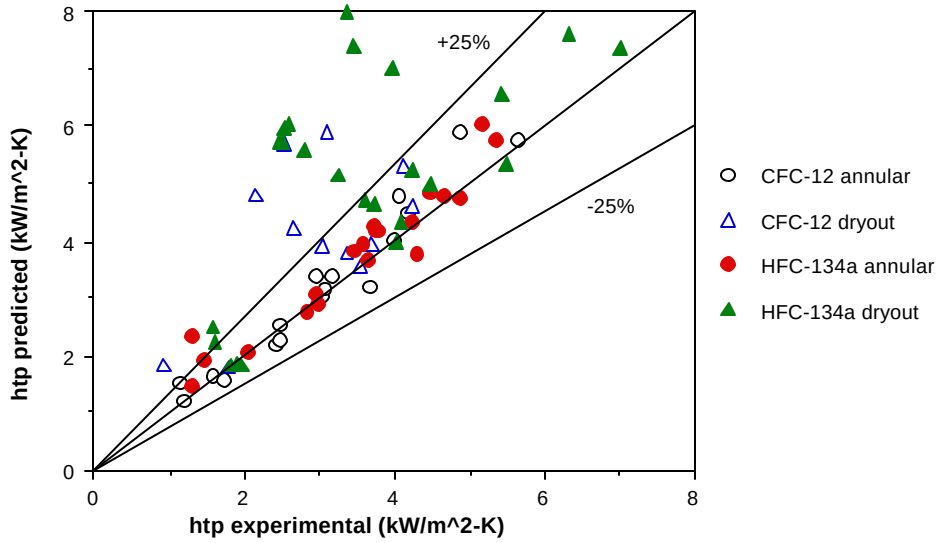

Figure 6.4. htp predicted by Jung et al. Correlation vs. htp experimental

6.2. Proposed Heat Transfer Correlation

Although the correlations previously available in the literature can predict the heat transfer with fair accuracy, still better accuracy may be desired. Most correlations contain terms which account for nucleate and convective boiling. But no correlations were found which account for the different flow patterns that may exist when a fluid is undergoing flow convective boiling.

A correlation is proposed for pure refrigerants which are flowing in an annular or wavy-annular flow pattern. Experimental data sets where dryout is observed on the top of tube at the exit of the test section are omitted. A correlation of the form proposed by Chaddock and Noerager (1966) is assumed:

$$\frac{h_{tp}}{h_l} = \frac{a}{(\chi_{tt})^b} \qquad (6.1)$$

When a regression analysis is performed on this form of the equation, the values of a and b which minimize the squares of the errors are a = 3.686 and b = 0.563. The mean deviation for CFC-12 was 11.7% and for HFC-134a was 8.7%. This correlation is plotted in Figure 6.1., along with the Chaddock-Noerager correlation.

Chapter 7: Conclusions and Recommendations

A test apparatus which measures heat transfer coefficients and pressure drops of evaporating refrigerants has been constructed and operated. Data were taken for both CFC-12 and HFC-134a in the automotive air conditioning range of flow rates, temperatures, and heat fluxes. Various oils were added to HFC-134a to determine any effect on heat transfer or pressure drop.

HFC-134a had higher heat transfer coefficients than CFC-12 at identical evaporation conditions. HFC-134a also had higher pressure drops than CFC-12. When three oils of similar viscosity were added to the HFC-134a, evaporative heat transfer coefficients generally increased for small oil concentrations, but decreased for larger oil concentrations. Pressure drops increased with increasing oil concentrations. There was no significant difference in heat transfer coefficient or pressure drop between the three different types of oil at identical concentrations.

The heat transfer coefficients for the pure refrigerants were compared with three correlations from the open literature. All three can predict the coefficients with fair accuracy for most tests. The prediction of htp for those tests where dryout occurs was not as accurate as for those tests where wavy-annular or completely annular flow was present. In order to obtain even greater accuracy for a smaller range of conditions, a new correlation is proposed.

More work in this area needs to be done in the future. Designers of evaporators need information on the heat transfer and pressure drop characteristics of the newer ozone-safe refrigerants and refrigerant-oil mixtures.

Some recommendations for future work are:

1) Obtain more local heat transfer coefficients, averaging over a smaller quality change. This can be done by considering a single thermocouple wall temperature and its associated bulk fluid temperature, and deriving the corresponding heat transfer coefficient for that location and flow quality.

2) Explore different refrigerants, oil mixtures, and tube geometries or enhancements. The basic heat transfer characteristics can be found from smooth circular tubes, but designers need more applied information.

3) Use the microcomputer to calculate heat transfer coefficients on line, instead of during post-test processing. This can help the operator identify interesting trends and perhaps schedule additional tests to explore those trends. This may be particularly useful in identification of flow regime transitions.

4) Obtain accurate information on the saturation temperature-pressure relationship of refrigerant-oil mixtures. Then set inlet or average test section temperatures or pressures according to the new equation when oil is mixed with the refrigerant.

5) Obtain accurate estimates of the non-ideal mixing behavior of refrigerant-oil combinations to be tested. The density of the real mixture can differ significantly from an ideal relation of component to mixture densities.

References

Aldhous, P., "Warming to Global Agreement," Nature, July 5, 1990, p. 6.

Chaddock, J. B., and J. A. Noerager, "Evaporation of Refrigerant 12 in a Horizontal Tube with Constant Wall Heat Flux," ASHRAE Transactions, Vol. 72, Part 1, 1966, pp. 90-101.

Dittus, F. W. and L. M. K. Boelter, Publ. Eng., Vol. 2, Univ. of California at Berkeley, 1930, p. 443.

Eckels, S. J., and M. B. Pate, "An Experimental Comparison of Evaporation and Condensation Heat Transfer Coefficients for HFC-134a and CFC-12," International Journal of Refrigeration, Vol. 14, 1991, pp. 70-78.

Eckels, S. J., and M. B. Pate, "In-Tube Evaporation and Condensation of Refrigerant-Lubricant Mixtures of HFC-134a and CFC-12," to be published in ASHRAE Transactions, Vol. 97, Part 2, 1991.

Fukushima, T., and M. Kudou, "Heat Transfer Coefficients and Pressure Drop for Forced Convection Boiling and Condensation of HFC 134a," Proceedings, ASHRAE-Purdue CFC Conference, 1990, pp.196-204.

Green, G. H., and F. G. Furse, "Effect of Oil on Heat Transfer from a Horizontal Tube to Boiling Refrigerant 12-Oil Mixtures," ASHRAE Journal, October, 1963, pp. 63-68.

Hambraeus, K., "Heat Transfer Coefficient, Two-Phase Flow Boiling of HFC134a," Proceedings, ASHRAE-Purdue CFC Conference, 1990, pp. 205-214.

Hambraeus, K., "Two Phase Flow Boiling of Oil-HFC134a Mixture," to be published in Proceedings, XVIIIth International Congress of Refrigeration, 1991.

Jung, D. S., and R. Radermacher, "Prediction of Heat Transfer Coefficient of Various Refrigerants During Evaporation," to be published in ASHRAE Transactions, Vol. 97, Part 2, 1991.

Jung, D. S., M. McLinden, R. Radermacher, and D. Didion, "A Study of Flow Boiling Heat Transfer with Refrigerant Mixtures," Int. J. Heat Mass Transfer, Vol. 32, No. 9, pp. 1751-1764, 1989.

Kandlikar, S. G. , "A General Correlation for Saturated Two-Phase Flow Boiling Heat Transfer Inside Horizontal and Vertical Tubes," Boiling and Condensation in Heat Transfer Equipment, HTD Vol. 85, pp. 9-19, New York, ASME, 1987.

Moffat, R. J., "Describing the Uncertainties in Experimental Results," Experimental Thermal and Fluid Science, Vol. 1, pp. 3-17, 1988.

Spatz, M. W., and J. Zheng, "An Experimental Evaluation of the Heat Transfer Coefficients of R-134a Relative to R-12," Proceedings, ASHRAE-Purdue CFC Conference, pp. 225-233, 1990.

Stephan, K., and M. Abdelsalam, "Heat transfer correlations for natural convection boiling," Int. J. Heat Mass Transfer, Vol. 23, pp. 73-87, 1980.

Takamatsu, H., S. Momoki, and T. Fujii, "A Comparison and Evaporation Heat Transfer Coefficients and Pressure Drop in a Horizontal Smooth Tube for HFC134A and CFC12," to be published in Proceedings, XVIIIth International Congress of Refrigeration, 1991.

Tichy, J. A., W. M. B. Duval, and N. A. Macken, "An Experimental Investigation of Heat Transfer in Forced-Convection Evaporation of Oil-Refrigerant Mixtures," ASHRAE Transactions, Vol. 92, Part 2A, 1986, pp. 450-460.

Wattelet, J. P., "Design, Building, and Baseline Testing of an Apparatus Used to Measure Evaporation Characteristics of Ozone-Safe Refrigerants," M. S. Thesis, University of Illinois at Urbana-Champaign, January, 1991.

Wattelet, J. P., J. C. Chato, J. M. S. Jabardo, J. S. Panek, and J. P. Renie, "An Experimental Comparison of Evaporation Characteristics of HFC-134a and CFC-12," to be published in Proceedings, XVIIIth International Congress of Refrigeration, 1991.

XingXi, Z., J. Xinqiao, X. Dazhong, and Y. Chibin, "Evaporation of R12 in a Horizontal Tube under the Refrigeration Condition," Proceedings, XVIIIth International Congress of Refrigeration, 1991.

Appendix A: Test Loop Start Up, Operation, and Shut Down

Test Loop Start Up

1) Make sure the "False Load Heater" and "Preheater" power disconnects are in the "OFF" position. Unplug the yellow power cable. Failure to perform this step will destroy the heaters when the computer is turned on!

2) Turn on the two instrument power supply strips. Turn on the refrigerant pump. Set the refrigerant pump control potentiometer to around "7" and wait to confirm refrigerant flow in the test section.

3) Unlock and open the computer security station and turn on the main power supply. Turn on the frequency counter on top of the computer station. Turn on the computer by pressing the button on top of the keyboard. When the computer has booted, select and run the application corresponding to the refrigerant in the test loop, for example, "Pure HFC-134a in TS#2" or "CFC-12 and 4GS oil in TS#3."

4) Make sure that all heater control settings are at 0 power on the worksheet (4 mA for Preheater and Test Section, and 0 VDC for False Load Heater control icons).

5) Throw "Preheater" and "Fals e Load Heater" power disconnects to the "ON" position. Plug in the yellow power cable. Throw "Chiller Compressor" and "Antifreeze Pumps and Test Section Heaters" disconnects to the "ON" position.

6) Open city water drain valve. Open city water supply valve. Make sure the city water pressure is at least 30 psig before proceeding.

7) Turn on the chiller power switch. Set the compressor setpoint temperature higher than the current antifreeze temperature. Turn on the antifreeze pump switch. Turn the TXV selection switch to the "LOW" position. Make sure the pumps are operating by checking the frequency counter display. It should be around 500 for warm antifreeze and as low as 75 for extremely cold antifreeze. A lower displayed frequency indicates possible failure of one of the pumps.

Test Loop Operation

1) A total of seven parameters must be set during a test run: false load heater power, preheater power, test section heater bank power, refrigerant pump speed, refrigerant pump bypass valve opening, refrigerant charge, and desired oil concentration. All heater power levels are controlled by the computer from settings in the Workbench‰ worksheet. Test section heater bank and preheater powers are off at settings of 4 mA and are on full power at settings of 20 mA. False load heater power is off at a setting of 0 VDC and is on full power at a setting of 10 VDC.

2) Several criteria must be met before logging data. Refrigerant flowing through the flow meter and into the preheater must be subcooled. Refrigerant at the inlet to the pump need not be subcooled, but two phase flow at this location is unsafe and should be avoided if possible by the addition of more charge to the test loop. The criteria on test conditions are as follows: Inlet quality to the test section within 1%, inlet temperature to test section within 0.5°C, mass flux in test section within 1%, heat flux in test section within 2%, and oil concentration within 0.1%.

3) Maintaining a desired antifreeze temperature is accomplished by setting the compressor setpoint temperature artificially low and adding sufficient false load heater power. When a change in false load heater power level is made, it takes at least 10 minutes before a steady temperature is achieved in the antifreeze and usually at least 20 minutes for refrigerant temperature to stabilize. Changes in preheater and test section heater power levels also affect equilibrium antifreeze temperature since the refrigerant test loop is thermally connected to the antifreeze loop.

The "HIGH" TXV valve gives the chiller higher cooling capacity at antifreeze temperatures higher than -20°C. The "HIGH" valve should never be used at antifreeze temperatures below -23°C, or liquid refrigerant might enter the compressor.

4) Mass flux in the test section is controlled by the pump speed potentiometer and pump bypass valve opening. Best operation is realized by running a high pump speed (potentiometer setting of 8 or 9) with sufficient bypass opening to achieve nearly the desired mass flux. Fine tuning of the mass flux is then done by adjusting the potentiometer. The highly sensitive potentiometer permits extremely fine control of the mass flux.

5) Quality of refrigerant entering test section is controlled by preheater power level. Quality is affected to a lesser degree by the amount of subcooling the refrigerant entering the preheater has.

6) Heat flux in the test section is controlled solely by the test section heater bank power level.

7) Inlet temperature to the test section is controlled mainly by the antifreeze temperature. It is also affected by the amount of charge in the loop and the preheater and test section heater bank power levels.

8) Refrigerant charge in the current configuration should be around 30 pounds for most tests. Adding or removing charge is useful when setting test section inlet temperature or maintaining sufficient subcooling before the preheater and refrigerant pump. Care must be taken to purge connecting hoses of air before adding refrigerant to the test loop. Add pure refrigerant as a vapor to the service port at the exit of the test section. Add any oil for testing to the service port at the inlet to the refrigerant pump. Remember that adding only refrigerant or only oil will alter the charge oil concentration. Removing charge will not alter the oil concentration if it is done from the service port at the inlet to the refrigerant pump when the charge is subcooled at that location. Let the test loop achieve equilibrium while taking out small amounts of charge, so that flow through the test section is not lost.

Test Loop Shut Down

1) Increase refrigerant pump speed to maximum and close bypass valve to within 1/4 turn of fully closed.

2) Turn off test section heater bank and false load heater power.

3) Set compressor setpoint temperature artificially high and wait for compressor to turn off. When antifreeze temperatures before and after the false load heater are equal, turn off the antifreeze pumps.

4) Reduce power level in the preheater gradually to zero power.

5) Set the refrigerant pump speed control to zero and turn off pump power.

6) Quit the Workbench™ application. When asked whether or not to save changes in the application, select "NO" in the dialog box.

7) Throw "Preheater" and "False Load Heater" power disconnects to the "OFF" position. Unplug the yellow power cable.

8) Close city water supply valve. Close city water drain valve.

9) Turn chiller control panel power switch to "OFF". Throw "Chiller Compressor" and "Test Section Heaters and Antifreeze Pumps" power disconnects to the "OFF" position.

10) Turn off frequency counter. Shut down the computer. Close and lock the computer security station.

Appendix B: Oil Charging, Concentration Measurement, and Flushing Procedures

Charging Test Loop with Oil

A commercial hand pump is used to inject oil into the test loop through the service port located at the refrigerant pump inlet. By keeping careful inventory of refrigerant in the test loop, it is easy to calculate the amount of oil needed to achieve a desired concentration. When the required volume of oil is estimated, the amount of pump strokes can be determined (46 mL / pump stroke).

Set the test loop up in thermal equilibrium so that a high flow rate of refrigerant at a moderate subcooling exists at the pump inlet.

Disassemble and clean the pump if a different type of oil is to be injected than the previous one. Rinse all metal parts with R-11 or some other solvent which the oil is soluble in. Clean all rubber gaskets and O-rings with a paper towel. Reassemble the pump.

Connect a clean hose from the pump outlet to the service port, but do not tighten it. Open the oil container and put the pump bottom into it. Work quickly if the oil absorbs water from the air. Adjust the retaining ring to secure the pump to the container.

Pump the plunger until air is displaced from the hose and oil begins to flow out the other end. Tighten the hose on the service port. Slowly move the plunger to the top of its stroke.

Open the service port all the way. Slowly pump the plunger from full up to full down. Moving the plunger very slowly will allow every stroke to draw a full volume (46 mL) of oil so that an accurate estimate can be made of the amount of oil added. Pump until the required amount of oil is added.

Close the service port and remove the hose. Remove the pump from the oil container. Close the oil container. Pump the plunger so that excess oil is discharged.

Circulate the refrigerant-oil mixture for at least an hour at moderately high temperature before attempting to measure the new concentration level.

Oil Concentration Measurement

The following procedure requires that the sample be extracted from a line that contains subcooled refrigerant. Set the test loop up in thermal equilibrium at a moderate refrigerant flow rate and a high pressure (700 kPa) at the preheater inlet. Adjust false load heater and preheater power levels so that refrigerant is subcooled at the preheater and refrigerant pump inlets. Measuring the oil concentration of the test loop charge is done according to the following procedure:

1) Clean the sampling container, shown in Figure 3.7., to remove water, dust, and oil from its outer surface. Try not to handle the container directly, but by holding it with a paper towel. Touching the surface can leave oils which the sensitive scale can detect.

2) Set the scale in a vibration and draft-free area and level it.

   Turn on power and let the electronics warm up. Wipe the scale pan to remove water or dust.

3) If the sampling container has more than around 50 grams of oil in it, disassemble and clean the inside of the container with R-11. Be sure to avoid getting R-11 inside the filter. Reassemble and tighten all fittings.

4) Evacuate the container through the gas port until the internal vacuum is around 30" Hg on the dial gage and no change in vacuum pump tone can be discerned when closing and opening the gas valve.

5) Zero the scale. Weigh the evacuated sampling cylinder and record the mass (M_1).

6) Connect a clean hose from the sampling container's liquid port to the service port before the refrigerant pump inlet. Open the liquid valve on the sampling container and evacuate the hose and container until the conditions in step 4 above have been met.

7) Close the gas valve and remove the vacuum source from the gas port. Close the container's liquid valve. Open the service port on the test loop fully open.

8) Try to get between 500 and 700 grams of sample. This can be done by opening the sampling container's liquid valve approximately 2 full turns and closing it again quickly.

9) Close the service port on the test loop. Loosen the connecting hose at the test loop end and allow the trapped liquid refrigerant and oil to escape. Remove the hose connection to the sampling cylinder.

10) Zero the scale. Weigh the cylinder and sample (M_2).

11) Connect a hose from the capillary valve to a recovery can submerged in an ice water bath. As with any refrigerant transfer operation, purge the hose of air with refrigerant vapor from the higher pressure vessel before tightening connections.

12) Open the capillary valve and allow the refrigerant in the sampling container to boil away and recondense in the recovery can. When pressure in the container approaches the saturation pressure at around 5°C, close the capillary valve and disconnect the recovery can. This step can take 2-5 hours depending on the initial sample size.

13) Connect the capillary valve to a vacuum source and evacuate through the capillary tube until a vacuum of 20" Hg exists in the sampling container.

14) Close the capillary valve and evacuate the container through the gas port until no change in vacuum pump tone can be discerned when opening and closing the gas valve. This last step is essential to the accuracy of the measurement, so make sure that all traces of refrigerant have been removed. This can sometimes take a while because the refrigerant is dissolved in the oil and boils out only very slowly.

15) Close the gas valve and disconnect the vacuum pump. Zero the scale and weigh the sampling container and oil from the sample (M_3).

16) The oil concentration is calculated by:

$$\omega_o = \frac{M_3 - M_1}{M_2 - M_1} \qquad \text{(sample basis)}$$

or

$$\omega_o = \frac{M_3 - M_1}{M_2 - M_3} \qquad \text{(refrigerant basis)}$$

Flushing Oil from the Test Loop

If there is a large difference in the normal boiling points of the refrigerant and oil, then the oil can be removed by distillation.

The current test loop design allows distillation of batches of charge. Briefly, a quantity of liquid refrigerant-oil mixture is removed from the test loop into a "dirty" recovery can. Pure refrigerant vapor is boiled out of the can

and condensed inside the test loop. Oil is left behind in the can. The process is repeated until a negligible concentration of oil is present in the test loop.

The procedure for doing this begins by setting the test loop up in thermal equilibrium with a moderate refrigerant flow rate. Set the preheater and false load heater power levels to achieve high pressure and subcooling at the service port located at the inlet to the refrigerant pump. Connect a hose from that port to the "dirty" can in an ice water bath. As with any refrigerant transfer operation, purge air from the hose before final tightening. Open the service port to remove a small quantity of charge and close it. Let the test loop regain equilibrium and observe the condition of flow in the sight glass. Continue removing small amounts of charge until the refrigerant is in a two-phase condition at the sight glass. At this time, turn the pump speed to maximum and begin slowly reducing the preheater power level to zero. Try not to lose flow through the test section, as it cools the preheater elements. Sudden loss of flow would thermally stress the preheater elements. If loss of flow occurs, immediately turn off power to the preheater.

After the preheater is turned off, turn the refrigerant pump off. Turn off the false load heater and let the chiller compressor run to lower pressure and temperature inside the test loop. Remove the "dirty" can from the ice bath and wipe away any water. Estimate the amount of charge removed to the nearest pound. Connect the can to the service port located at the end of the test section. Purge the hose of air.

Open the service port and the can valve to allow refrigerant to boil out of the can and condense in the test loop. Running the chiller to cool the test loop and heating the can with a heat gun or tape heater will speed up this process. Weigh the can periodically. When most of the refrigerant has boiled away, repeat the process of extracting oily refrigerant as above.

Exact concentrations can be measured to confirm the effect of oil removal. A less accurate but faster approximation of the oil concentration can be obtained by keeping track of the amount of refrigerant purified in each batch. Assuming all oil is removed from each batch and only pure refrigerant is returned to the test loop, the concentration (ω_o) after N batch distillations is:

$$(\omega_O)\text{final} = \frac{(\omega_O)\text{initial}}{(IC)^N} * \prod_{i=1}^{N}(IC\text{-}R_i)$$

where IC is the initial charge of refrigerant and R_i is the amount of refrigerant purified in each batch. For example, assume an initial charge of 50 pounds and concentration of 5%. Four batches are distilled, with 16, 15, 18, and 17 pounds purified in each batch. The final concentration is 1.005%:

$$(\omega_O)\text{final} = \frac{5}{(50)^4} * (34) * (35) * (32) * (33)$$

In the above example, refrigerant should be added so that a larger fraction of the total charge can be purified in each step. Obviously more batches need to be distilled before the remaining oil can be considered negligible.

Appendix C: Test Conditions and Results

Table C.1. Conditions and Results of Pure CFC-12 Tests

Heat Flux (kW/m^2)	Mass Flux (kg/m^2s)	Inlet X (%)	Outlet X (%)	Date	Run #	h (W/m^2K)	dP (kPa)
5.0	105	19.2	49.7	10/3/91	1	1185	0.4
5.0	102	39.8	71.0	10/3/91	2	1149	0.6
5.0	98	61.7	94.3	10/3/91	3	922	0.7
5.0	294	10.3	21.3	10/5/91	5	1570	1.3
5.0	300	20.5	31.2	10/3/91	4	2428	2.4
5.0	303	39.9	50.5	10/3/91	6	3086	5.5
4.9	296	60.8	71.5	10/3/91	8	3707	8.3
4.9	503	10.3	16.6	10/5/91	6	2466	3.3
5.0	492	20.3	26.8	10/3/91	5	3050	6.6
4.9	503	39.0	45.3	10/3/91	7	4184	14.2
5.0	497	59.6	66.0	10/3/91	9	5654	19.6
9.8	100	20.4	83.2	10/2/91	6	1741	0.7
9.9	101	38.5	100.0	10/2/91	7	1788	0.9
9.9	301	19.7	40.8	10/2/91	1	2465	3.4
9.8	298	40.3	61.4	10/2/91	3	3169	6.3
10.0	305	59.4	80.3	10/2/91	4	2654	7.0
10.0	304	78.8	99.8	10/2/91	8	2141	6.9
9.9	503	20.0	32.6	10/2/91	2	2943	8.4
10.0	500	39.9	52.7	10/2/91	5	4051	16.2
10.1	501	57.8	70.7	10/4/91	1	4854	19.4
20.0	297	20.3	63.5	10/7/91	2	3662	5.8
20.0	300	40.1	82.8	10/4/91	4	3033	7.1
20.0	502	19.6	45.1	10/7/91	1	3991	11.9
20.0	501	40.3	65.9	10/4/91	3	4123	16.3
20.0	495	51.0	76.9	10/4/91	2	3112	14.6
25.4	307	19.3	72.4	10/5/91	1	3559	5.9
30.3	303	18.8	82.8	10/5/91	2	3360	6.5
29.7	500	19.7	57.7	10/5/91	3	4228	13.4
30.0	502	39.4	77.7	10/5/91	4	2529	14.3

Table C.2. Conditions and Results of Pure HFC-134a Tests

Heat Flux (kW/m^2)	Mass Flux (kg/m^2s)	Inlet X (%)	Outlet X (%)	Date	Run #	h (W/m^2K)	dP (kPa)
4.9	98	24.8	49.3	7/10/91	1	1318	0.5
5.1	106	38.7	62.6	7/10/91	2	1462	0.9
4.8	105	61.0	83.9	7/10/91	3	1307	1.1
5.2	299	21.1	29.9	7/4/91	6	2833	3.1
5.0	305	39.3	47.9	7/4/91	5	3594	6.8
5.0	295	60.7	69.7	7/4/91	4	4481	9.7
5.0	500	19.7	25.5	7/4/91	1	3457	8.4
4.9	501	39.6	45.9	7/4/91	2	5337	17.0
4.9	495	59.6	65.9	7/4/91	3	7006	21.3
10.2	104	20.3	68.8	7/1/91	1	1916	1.0
10.3	103	18.9	68.9	7/3/91	2	1963	1.0
10.1	102	19.9	68.9	9/19/91	2	1906	0.8
10.1	99	21.0	71.4	9/30/91	1	1809	0.8
10.2	104	39.7	87.7	7/1/91	2	1602	1.3
10.0	106	54.5	99.7	7/1/91	3	1597	1.5
10.2	137	20.1	57.0	7/10/91	7	2063	1.4
10.2	271	19.9	38.8	7/10/91	6	2971	3.4
10.2	305	20.0	36.9	6/20/91	1	2956	4.0
10.0	302	40.1	56.9	6/20/91	2	3729	7.7
10.0	300	59.5	76.3	6/20/91	3	4234	9.8
10.4	300	79.9	97.2	6/20/91	4	2611	8.9
10.2	402	20.4	33.5	7/10/91	5	3631	6.9
10.2	510	19.5	30.1	6/10/91	1	3778	9.8
10.2	499	20.1	31.1	9/12/91	1	3776	9.9
10.2	502	39.7	50.9	6/10/91	2	5151	18.0
10.2	497	59.5	71.0	6/28/91	1	6333	22.1
10.1	537	19.7	29.8	7/10/91	4	4241	11.0
19.7	308	20.5	52.4	6/30/91	2	4293	6.4
19.4	294	39.6	72.7	6/30/91	3	3744	7.8
20.3	301	39.5	73.3	9/12/91	2	3613	7.6
19.3	299	59.3	91.6	6/30/91	4	2816	8.6
19.3	302	69.7	100.0	6/30/91	5	2532	9.1
19.9	498	20.6	41.4	6/25/91	1	4468	13.1
20.6	491	20.1	41.8	6/30/91	1	4666	13.0
19.8	503	19.7	39.1	9/30/91	2	4879	13.0
20.5	500	40.0	61.6	6/25/91	2	5444	20.6
20.3	487	61.3	82.9	6/25/91	3	3371	18.1
24.1	298	20.0	60.1	6/19/91	1	4035	6.3
26.3	314	52.8	94.0	7/3/91	3	2470	9.2
24.5	310	55.5	94.7	7/3/91	5	2521	8.9
24.4	498	49.4	74.7	7/3/91	4	3458	17.0
29.3	301	20.1	68.5	7/2/91	1	4092	7.3
29.1	298	39.6	88.3	7/2/91	2	3265	8.5
29.2	496	19.6	49.7	7/2/91	3	5500	15.6
30.9	504	39.3	70.6	7/2/91	4	3972	17.2

Table C.3. Conditions and Results of HFC-134a / 1% PAG 0332 Mixture Tests

Heat Flux (kW/m^2)	Mass Flux (kg/m^2s)	Inlet X (%)	Outlet X (%)	Date	Run #	h (W/m^2K)	dP (kPa)
5.0	107	20.0	43.2	7/20/91	1	1785	0.6
5.0	103	40.7	64.8	7/20/91	2	1876	1.1
4.9	108	57.7	80.6	7/20/91	3	1876	1.8
5.0	296	21.0	29.6	7/20/91	4	3029	3.1
4.9	297	40.7	49.3	7/20/91	5	4229	7.6
4.9	301	60.1	68.7	7/20/91	6	5560	11.7
5.2	502	20.3	26.2	7/22/91	1	4580	10.3
5.1	499	40.2	46.6	7/22/91	2	7033	18.4
5.1	499	44.6	51.0	7/22/91	3	6774	19.5
9.9	100	20.5	68.9	7/15/91	1	2079	1.1
10.1	106	38.9	85.9	7/15/91	2	2277	1.6
9.9	297	20.6	37.2	7/19/91	1	3119	4.1
10.0	297	39.7	56.8	7/19/91	2	4297	8.7
10.2	293	60.2	78.0	7/19/91	3	5647	12.5
10.2	498	19.7	30.7	7/12/91	1	5207	11.7
10.2	498	37.9	49.4	7/15/91	3	6258	19.7
20.6	296	20.5	55.1	7/11/91	1	5646	8.0
19.5	302	40.0	72.6	7/11/91	3	5248	11.9
19.1	301	60.1	92.0	7/15/91	5	4758	14.0
19.1	502	19.8	39.8	7/11/91	2	5360	15.4
19.3	504	19.9	39.8	7/18/91	1	5173	15.3
19.0	496	31.9	52.2	7/15/91	4	6040	20.9

Table C.4. Conditions and Results of HFC-134a / 3% PAG 0332 Mixture Tests

Heat Flux (kW/m^2)	Mass Flux (kg/m^2s)	Inlet X (%)	Outlet X (%)	Date	Run #	h (W/m^2K)	dP (kPa)
5.1	98	21.0	46.5	7/27/91	1	2256	0.7
5.2	98	41.2	66.9	7/27/91	2	2087	1.4
5.1	102	59.3	83.9	7/27/91	3	1566	2.2
5.1	296	20.6	29.3	7/27/91	4	2815	3.4
4.9	298	40.1	48.7	7/30/91	1	4523	7.8
4.8	296	60.3	69.1	7/30/91	3	4605	11.8
4.9	500	20.0	25.6	7/30/91	2	5441	10.5
4.9	497	39.6	45.8	7/30/91	4	6540	18.8
4.9	492	45.0	51.3	7/31/91	1	7502	20.4
10.0	103	21.8	68.8	7/26/91	8	1708	1.4
9.8	90	44.9	94.9	7/26/91	7	3363	1.9
9.8	300	20.4	36.8	7/26/91	2	3839	5.0
10.1	301	39.7	56.6	7/26/91	3	4229	9.3
9.8	295	59.1	76.1	7/26/91	4	4022	13.0
9.7	496	20.4	30.9	7/26/91	5	5286	13.1
10.2	509	39.2	50.5	7/26/91	6	6579	21.7
20.7	303	20.2	54.1	7/26/91	1	5109	8.9
20.3	297	39.6	73.5	7/25/91	4	5182	13.4
19.2	289	61.9	95.0	7/25/91	3	3670	18.6
20.2	499	20.2	40.4	7/25/91	1	5675	17.5
19.1	499	29.7	49.9	7/25/91	2	6478	22.4

Table C.5. Conditions and Results of HFC-134a / 5% PAG 0332 Mixture Tests

Heat Flux (kW/m^2)	Mass Flux (kg/m^2s)	Inlet X (%)	Outlet X (%)	Date	Run #	h (W/m^2K)	dP (kPa)
5.0	102	20.0	44.1	9/7/91	1	2422	0.7
5.0	97	41.3	66.9	9/7/91	2	2008	1.2
5.0	103	57.1	81.0	9/7/91	3	1558	2.2
5.0	297	20.1	28.7	8/1/91	1	2439	3.5
5.1	296	40.0	49.1	8/1/91	2	3466	7.9
5.2	305	59.1	68.3	8/1/91	3	3391	12.6
5.2	493	20.6	26.7	8/2/91	1	5353	11.5
4.9	500	40.7	46.9	9/7/91	7	4849	19.3
5.0	498	45.0	51.5	9/8/91	2	7313	20.4
10.2	105	20.0	67.7	8/2/91	7	1168	1.5
10.1	99	41.1	91.1	8/2/91	6	1903	2.9
10.0	296	19.8	36.7	9/7/91	4	3601	5.0
9.9	297	41.0	58.0	9/7/91	6	3428	9.6
10.1	299	59.5	77.0	8/2/91	4	3308	14.9
10.4	499	20.0	31.3	8/2/91	2	4885	13.7
9.8	498	40.5	51.8	9/8/91	3	6762	22.1
19.7	297	20.0	53.2	9/7/91	5	4731	8.8
20.3	303	40.4	74.2	8/2/91	5	4192	15.1
19.5	303	58.4	90.8	9/7/91	8	3131	21.0
20.3	503	19.9	41.1	8/2/91	3	5588	18.0
19.9	497	30.3	51.6	9/8/91	1	6138	23.4

Table C.6. Conditions and Results of HFC-134a / PAG 0354 Mixture Tests

Oil Conc. (%)	Heat Flux (kW/m^2)	Mass Flux (kg/m^2s)	Inlet X (%)	Outlet X (%)	Date	Run #	h (W/m^2K)	dP (kPa)
1.0	5.1	99	40.8	66.3	9/23/91	2	2058	0.8
1.0	10.1	301	19.8	36.5	9/23/91	1	3449	3.8
1.0	20.0	300	19.6	52.7	9/23/91	3	5149	7.0
1.0	10.1	297	41.1	58.3	9/23/91	4	5012	8.8
1.0	10.1	294	61.2	78.7	9/23/91	5	6138	11.7
1.0	20.0	496	20.5	41.3	9/23/91	6	5420	15.1
3.0	4.6	99	21.2	44.1	9/24/91	1	1852	0.5
3.0	10.1	301	19.7	36.7	9/24/91	2	3811	4.6
3.0	20.2	304	19.9	53.2	9/24/91	3	5077	8.5
3.0	10.1	302	40.1	57.2	9/24/91	4	4206	9.2
3.0	9.8	299	60.5	67.5	9/24/91	5	4786	13.0
3.0	19.6	501	20.1	33.5	9/24/91	6	5726	16.7
5.0	5.1	100	40.2	65.1	9/25/91	1	2203	1.2
5.0	10.1	297	20.0	36.7	9/25/91	2	3425	5.0
5.0	19.9	303	19.9	52.3	9/25/91	6	4743	9.4
5.0	10.0	301	39.7	56.0	9/25/91	3	3867	9.4
5.0	9.9	300	59.3	75.5	9/25/91	4	3920	14.4
5.0	19.9	503	19.8	39.2	9/25/91	5	5623	17.0

Table C.7. Conditions and Results of HFC-134a / Ester 0540 Mixture Tests

Oil Conc. (%)	Heat Flux (kW/m^2)	Mass Flux (kg/m^2s)	Inlet X (%)	Outlet X (%)	Date	Run #	h (W/m^2K)	dP (kPa)
1.0	5.1	101	39.6	64.8	9/13/91	1	1571	0.9
1.0	10.0	299	20.0	36.7	9/13/91	2	3240	3.9
1.0	19.9	296	20.2	53.7	9/13/91	3	4472	7.1
1.0	10.1	300	39.7	56.9	9/13/91	4	4143	8.7
1.0	10.1	295	60.9	78.3	9/13/91	5	3400	9.8
1.0	19.8	499	20.3	40.9	9/13/91	6	4414	13.7
3.0	5.0	101	39.7	64.1	9/14/91	1	2152	1.1
3.0	9.8	298	19.8	36.4	9/14/91	2	3949	4.5
3.0	19.3	300	20.1	52.3	9/14/91	3	5564	8.2
3.0	9.8	298	40.7	57.5	9/14/91	4	4614	9.1
3.0	9.8	299	59.0	75.7	9/14/91	6	5441	12.5
3.0	19.7	501	20.3	40.8	9/14/91	5	5746	16.5
5.0	5.0	99	20.5	45.2	9/17/91	1	2477	0.6
5.0	5.3	108	38.4	63.2	9/15/91	1	2326	1.4
5.0	9.9	302	20.1	36.8	9/15/91	2	3789	5.0
5.0	19.5	307	19.6	51.6	9/15/91	3	5058	8.7
5.0	10.0	304	38.9	55.7	9/16/91	1	3955	9.4
5.0	10.0	292	61.1	78.6	9/16/91	3	3965	12.9
5.0	20.5	505	19.5	40.6	9/16/91	2	5785	17.1
5.0	20.0	499	40.3	61.5	9/17/91	2	6578	25.2